

(Proposal PR06-005 to Jefferson Lab PAC 29)

Parity Violating Electron Scattering in the Resonance Region (Res-Parity)

December 6, 2005

P. E. Bosted (spokesperson), E. Chudakov, V. Dharmawardane (co-spokesperson), A. Deur, R. Ent
D. Gaskell, J. Gomez, M. Jones, R. Michaels, B. Reitz, J. Roche, B. Wojtsekhowski
Jefferson Lab, Newport News, VA 23606

J. Arrington (co-spokesperson), K. Hafidi, R. Holt, H. Jackson, D. Potterveld,
P. E. Reimer, X. Zheng (co-spokesperson)
Argonne National Lab, Argonne, IL 60439

W. Boeglin, P. Markowitz
Florida International University, Miami, FL 33199

M.E. Christy, C. Keppel
Hampton University, Hampton, VA 23668

E. Hungerford
University of Houston, Houston, TX

G. Niculescu, I. Niculescu
James Madison University, Harrisonburg, VA 22807

T. Forest, N. Simicevic, S. Wells
Louisiana Tech University, Ruston, LA 71272

E. J. Beise, F. Benmokhtar
University of Maryland, College Park, MD 20742

K. Kumar, K. Paschke
University of Massachusetts, Amherst, MA 01003

F. R. Wesselmann
Norfolk State University, Norfolk, VA

Y. Liang, A. Opper
Ohio University, Athens, Ohio 45701

X. Jiang
Rutgers University, Rutgers, NJ 08544

P. Decowski
Smith College, Northampton, MA 01063

R. Holmes, P. Souder
University of Syracuse, Syracuse, NY 13244

D. Armstrong
College of William and Mary, Williamsburg, VA

S. Connell, M. Dalton
University of Witwatersrand, Johannesburg, South Africa

R. Asaturyan, H. Mkrtchyan (co-spokesperson), T. Navasardyan, V. Tadevosyan
Yerevan Physics Institute, Yerevan, Armenia

and the Hall A Collaboration

Abstract

We propose to perform the first measurements of the parity violation (PV) asymmetries A_p , A_d , and A_C over the full resonance region ($1 < W < 2.1$ GeV) at $Q^2 \approx 0.8$ GeV². The measurements consist of scattering 4.8 GeV longitudinally polarized electrons from unpolarized hydrogen, deuterium, and carbon targets at a scattering angle centered on 12.5 degrees, using the HRS-L and HRS-R spectrometers in Hall A. The projected total asymmetry errors are approximately 4–6% (relative) for hydrogen and 3–4% for the deuteron and carbon in each of four regions in W . Averaging the results over the full W range, the overall error is projected to be about 3% for hydrogen, 2.5% for deuterium and carbon (including a 1.8% systematic uncertainty which largely cancels between targets), and the errors on the ratios A_p/A_d and A_C/A_d are projected to be about 3.5% (dominated by statistical uncertainties).

The goals include the study of resonance structure in A_p and A_d , and exploring both global and local quark-hadron duality with the previously un-studied combination of structure functions probed by PV inelastic electron scattering. The carbon target allows an investigation of the EMC effect that emphasizes the flavor dependence and valence vs. sea contributions. The PV asymmetry is particularly sensitive to the isospin decomposition, as well as the axial hadronic current.

The results are of great practical importance in more accurately modeling neutrino interactions in the few GeV region, which is essential in the interpretation of neutrino oscillation experiments. The new data are also needed for modeling of radiative corrections to PV in the DIS region, and will also help in understanding backgrounds for other PV experiments.

The experiment will use the same Compton polarimeter, targets, detectors, and electronics as the planned experiment E05-007 (DIS-parity). The use of a lower beam energy (4.8 GeV compared to 6 GeV) is the only essential difference. We request a total of 29 days for production running and 1 day for checkout and calibrations.

Contents

I. Introduction and Motivation	4
A. Physics Overview	4
B. Impact on other Parity Violating Electron Scattering Measurements	5
C. Impact on Neutrino Scattering Measurements	6
II. Physics	6
A. Parity Violating Asymmetry - Formalism	6
1. Resonance Region Asymmetry	7
2. Deep-Inelastic Asymmetry	8
B. Physics of the Proton Measurements	9
1. Parity Violating Response in the Resonance Region	10
2. Duality	11
C. Nuclear Targets	13
1. Duality and Higher Twist	13
2. EMC ratios	14
D. Impact on other measurements	15
III. Experiment	16
A. Optimization of Kinematics	16
B. Beam Line and Polarimetry	17
C. Parity DAQ (Hall A)	17
D. The Liquid Target	17
E. Luminosity Monitor	18
F. Spectrometers and Pole-tip Background	18
G. Particle Identification Detectors	19
H. Fast Counting DAQ	19
1. FADC-based DAQ	19
2. Scaler-based DAQ	21
IV. Expected Results	21
A. Kinematic Coverage	21
B. Statistical and Systematic Uncertainties	22
C. Beam Polarization	22
D. Kinematic determination of Q^2	23
E. Electromagnetic Radiative Corrections	24
F. Electroweak Radiative Corrections	25
G. Beam Asymmetries	25
H. Pion Contamination	25
I. Pair Symmetric Background	25
J. Target Related Systematics	26
V. Request	26
VI. Physics Summary	27
VII. Collaboration	27
Appendix A. E04-101: G0 Backward Angle Measurement	27
Appendix B. E05-007: $\bar{e}-^2\text{H}$ Parity Violating Deep Inelastic Scattering at CEBAF 6 GeV	30
References	30

I. INTRODUCTION AND MOTIVATION

The electromagnetic interaction has proved very successful in probing the structure of the nucleon. Inelastic electron scattering at high momentum transfer Q^2 and excitation energy ν (corresponding to large missing mass W) has provided the best information to date on the parton distribution functions, whose universal nature makes them useful in understanding a wide variety of particle interactions with nucleons. One limitation is that spin-averaged inclusive electron scattering probes quarks weighted by their charge squared. For a proton target this means that there is no differentiation between quarks and anti-quarks, and that the contribution from down and strange quarks is strongly suppressed relative to the up quarks. Our best information on the down quark PDFs come from using a neutron target, although at high momentum fraction $x = Q^2/2M\nu$ (where M is the nucleon mass), corrections from nuclear binding (Fermi motion) become large. Because the weak charges of the strange and down quarks are relatively larger than the electromagnetic ones, the weak interaction can provide another sensitive means to probe the down and strange PDFs.

An alternative basis for the description of nucleon excitations is in terms of transition form factors to specific resonant states. Lately, the subject of quark-hadron duality has received considerable interest, both theoretically and experimentally. Theoretical interest comes about in making a unified QCD description of the hadronic interactions. Experimental interest arises because to the extent that duality works, it can be used to extract both spin-averaged and spin-dependent PDFs at large x . Duality is also of great importance experimentally to predict cross sections in regions where they haven't been measured precisely (for example, in predicting neutrino scattering cross sections needed to interpret neutrino oscillation experiments). The weak neutral current gives access to the axial hadronic current, which also enters in weak charge current interactions.

There are some data available in the DIS region, and more recent, high precision measurements for elastic e - p scattering, but there are no data available in the resonance region and very little data for heavy ($A > 2$) targets. The proposed measurements on hydrogen, deuterium and carbon will provide measurements over the entire resonance region, allowing studies of duality, higher twist, and nuclear effects in the parity violating response. Such data will also be important as input to future parity violation electron scattering measurements planned for the JLab 12 GeV upgrade, as well as input to upcoming low-to-moderate energy neutrino-nucleus scattering measurements.

All of these observations suggest that it is long overdue to measure the PV asymmetry A_p , A_d , and A_C in inelastic electron scattering at low Q^2 . JLab is the only laboratory with sufficient beam energy and intensity to make these measurements in a meaningful way.

A. Physics Overview

Electron scattering measurements sensitive to the weak neutral current are quite limited. The pioneering experiment of Prescott *et al.* [1, 2] using inelastic scattering on the deuteron helped establish the standard electroweak model. The relatively large errors on the parity-violating asymmetry A_d measured in the Prescott *et al.* experiment are no longer relevant in constraining physics beyond the Standard Model, or in constraining the strange quark PDFs. The experimental program at HERA at very high Q^2 (comparable to M_Z^2 , where M_Z is the Z -boson mass) are of limited statistical precision.

While previous measurements have focused on DIS measurements, the study of the resonance region is also of significant interest. New measurements at Jefferson Lab have allowed us to probe the resonance region in great detail, providing both high precision measurements over a large kinematic region, but also providing new information by allowing us to separate the longitudinal and transverse responses [3], as well as measuring the polarized structure functions in the resonance region [4]. These measurements provide additional information on resonance structure, beyond what is known from measurements of F_2 . Because of the much different isospin structure and different couplings, the weak current will couple to individual resonances differently than the electromagnetic current, which can help in identifying new or poorly established resonances.

In the quark-hadron duality picture, the response averaged over resonances should equal that at higher Q^2 , once target mass corrections and leading-log effects are taken into account [5–7]. Duality in

inclusive scattering has been observed in the unpolarized structure function, the separated longitudinal and transverse structure functions, and in the spin structure function [8]. Duality in the unpolarized F_2 structure function is satisfied to $\sim 5\%$ down to $Q^2=0.5 \text{ GeV}^2$, and we will be able to make tests of local duality with comparable precision, and global duality down to 2-3%. If duality is observed to hold at this level, it would imply small higher twist corrections which would be of great benefit for measurements at 6 and 12 GeV designed to access strange quark distributions, the $d(x)/u(x)$ ratio at large x , or look for physics beyond the standard model. However, models of quark-hadron duality have predicted quantitative differences between the level of duality for unpolarized, polarized, and parity violating response functions [9], as well as differences for the proton and the neutron [10]. Since no measurements exist at present, it is possible that surprises await, and that deviations from the leading order picture could be significant.

One can also study duality and make estimates of higher twist contributions for the nuclear targets. This is particularly relevant as input to neutrino scattering measurements, which use nuclear targets, or future parity violating electron scattering measurements that use isoscalar targets to make standard model tests. Since most neutrino experiments use nuclear targets, it is especially important to understand how the EMC effect changes the effective u and d quark distributions individually (or equivalently the isospin decomposition of the nucleon resonances). Unpolarized electron scattering is dominated by the effective u quark distributions at high x , while PV electron scattering has a large sensitivity to the effective d quark distributions. This makes PV electron scattering data a new way to help separate the quark-dependence of the EMC effect and look for differences between quark flavors or valence and sea quarks [11–13].

Most recent electron PV experiments have focused on elastic channels, with the goal of probing the strange quark form factor of the nucleon (SAMPLE at Bates, HAPPEX and G0 at JLab, A4 at Mainz, etc.), and ultimately searching for physics beyond the standard Model (QWeak and DIS-parity at JLab). The proposed measurements are complementary to the elastic and DIS measurements, providing a first look over the resonance region for proton, deuteron, and carbon targets. The only other planned measurement in the resonance region is E04-101, which will run in parallel with the G0 backward angle proton measurements. The G0 experiment will study parity violation in the region from pion threshold to the peak of the $\Delta(1232)$ resonance for Q^2 centered on 0.6 GeV^2 at a large scattering angle (centered around 110 degrees). See Appendix A for more details. Combining the G0 data with the forward angle data of this proposal at similar Q^2 will allow a Rosenbluth separation to be made in a limited range of W for a proton target. In addition to providing an approximately seven-fold increase in W range and data on three targets instead of one, the proposed measurements will provide input to improve future measurements, as detailed in the following sections.

B. Impact on other Parity Violating Electron Scattering Measurements

The DIS-parity experiment (E05-007) was approved by a previous PAC to make a Phase I measurement on deuterium in the DIS region at 6 GeV ($Q^2=1.1 \text{ GeV}^2$, $W^2=4.2 \text{ GeV}^2$ and $Q^2=1.9 \text{ GeV}^2$, $W^2=5.3 \text{ GeV}^2$). See Appendix B for more details. With an 11 GeV electron beam at JLab, or a 30 GeV beam at SLAC, it will be possible to repeat the original Prescott experiment with more than an order-of-magnitude reduction in error bars. This will allow a competitive search for new physics, or to establish coupling of new particles if they have already been found at LHC. One hint that such new physics may exist comes from the observation of a 3-sigma discrepancy with the Standard Model from the NuTeV neutrino scattering experiment at Fermilab [14, 15]. However, conventional explanations of this discrepancy also exist, for example a particle-antiparticle asymmetry in the strange sea, charge symmetry violation, or higher twist corrections [16, 17].

The interpretation of new high-precision measurements of parity violating electron scattering will rely on a reasonable understanding of scattering at lower energy and W , through radiative effects. If a given experiment measures electron scattering with incident energy E_0 and scattered electron energy E'_0 , the helicity-dependent cross sections must be known at all incident energies $E > E'_0$ and all scattered electron energies $E'_0 < E' < E_0$. For $E_0 = 11 \text{ GeV}$, E'_0 will typically be 3 to 5 GeV (see JLab 12 GeV pCDR), so measurements are needed down to $E = 3 \text{ GeV}$. These data will also allow for improved

radiative corrections for the 6 GeV DIS-parity measurement.

Lower energy data will also be crucial to understand the role of higher twist corrections, which are generally expected to decrease with powers of Q^2 and/or W^2 . Measurements over a large range of Q^2 and W are needed to constrain higher twist diagrams, because there are no models to calculate them reliably. The proposed experiment will provide a measurement of higher twist contributions a factor of two more precise than the approved DIS-parity measurements for $x \approx 0.3$ on deuterium. We will provide similar quality measurements over a range in x for hydrogen and carbon as well as deuterium.

Finally, parity violating scattering in the inelastic region is a background for other measurements, such as the SLAC E158 measurement of parity violating Møller scattering. For their measurement, the inelastic background from electron-proton scattering provided the largest correction to the measured e - e asymmetry, as well as the largest single systematic uncertainty. Dealing with these backgrounds will clearly be a crucial issue for the envisioned measurements of the Møller asymmetry at 12 GeV, which aims to be much more precise than the SLAC results.

C. Impact on Neutrino Scattering Measurements

A better understanding of the weak interaction at low Q^2 (1 to 3 GeV²) is of great importance in understanding low energy neutrino interactions, which in turn are needed to determine neutrino masses and couplings through neutrino oscillation experiments [18–21]. Neutrino oscillations in the channel $\nu_\mu \rightarrow \nu_\tau$ will be studied by τ production from neutrinos at underground neutrino telescopes like AMANDA, ANTARES, BAIKAL, and NESTOR, and with long base-line accelerator experiments like ICARUS, MINOS, MINER ν A, MONOLITH, and OPERA. Future high-accuracy experiments such as NO ν A and T2K will require even better knowledge of neutrino cross sections. In most experiments, the neutrinos have sufficient energy so that the excitation of nucleon resonances is possible. To go from the τ yield to incident neutrino flux, one needs accurate predictions for the cross section integrated over the neutrino energy spectrum. This involves the three charged current structure functions W_1 , W_2 , and W_3 . Using isospin symmetry, W_1 and W_2 can be related to measurements using inclusive unpolarized electron scattering, and essentially depend on a knowledge of the hadronic vector current. PV electron scattering places additional constraints on the structure functions because of the very different weighting of isoscalar and isovector amplitudes compared to unpolarized scattering. Spin-averaged scattering is highly dominated by the u quarks, while PV scattering has relatively strong d quark contributions. Also, PV scattering is somewhat sensitive to the axial nucleon current. Modeling of neutrino cross sections requires assumptions such as PCAC to relate vector and axial currents that may break down with increasing energy, so experimental constraints from PV scattering are useful [21–24]. The role of duality in the weak current has been discussed in the literature [19, 25, 26], and can be tested with the present proposal.

Our proposed measurements at the 4% level for twelve roughly evenly spaced W values from threshold through the resonance region and slightly into the DIS region ($W = 2.1$ GeV) will provide powerful constraints on the models used to predict the neutrino cross sections, and complement the direct measurements planned at MINER ν A [19].

II. PHYSICS

A. Parity Violating Asymmetry - Formalism

Figure 1 shows the lowest-order Feynman diagrams for inelastic lepton-nucleon scattering for electromagnetic and weak interactions. Electrons can scatter from protons by exchanging either a virtual photon, γ^* , or a Z^0 . Therefore the cross section for lepton-nucleon scattering can be written as,

$$d\sigma = d\sigma_\gamma + d\sigma_{weak} + d\sigma_I, \quad (1)$$

where $d\sigma_\gamma$ is the electromagnetic, $d\sigma_{weak}$ is the weak and $d\sigma_I$ is the interference contributions to the total cross section. For low-energy small-momentum-transfer lepton-nucleon scattering, the weak cross

section is much smaller than the electromagnetic cross section, so the former can be safely neglected. However, the electromagnetic part is parity conserving, so the cross section is the same for right and left handed electrons, while the neutral current amplitude contains a parity violating term. Consequently the weak neutral current can be measured using the parity-violating asymmetry in the inclusive cross sections for electrons polarized parallel (R) and anti-parallel (L) to their momentum. The PV asymmetry is given by

$$A_{RL} = \frac{d\sigma_R - d\sigma_L}{d\sigma_R + d\sigma_L}. \quad (2)$$

Here $d\sigma_R$ and $d\sigma_L$ are the cross sections for scattering right and left handed electrons off an unpolarized target.

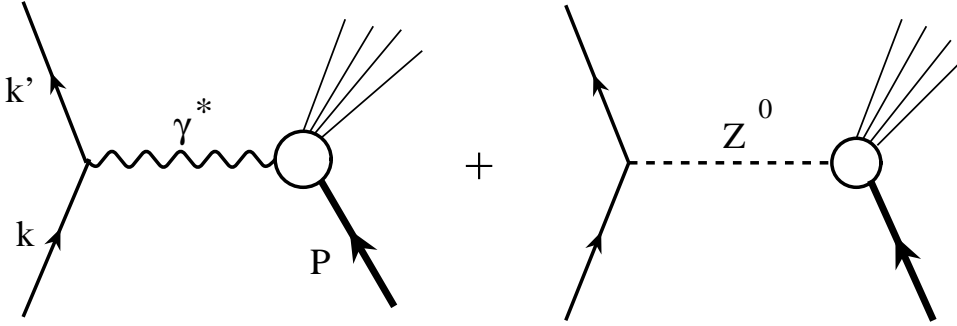


FIG. 1: First order Feynman diagrams for lepton-nucleon scattering in the presence of a weak neutral current.

1. Resonance Region Asymmetry

In the nucleon resonance region, it is possible to describe A_{RL} in terms of response functions to specific final states, combined with a non-resonant background. In the one gauge boson (γ or Z^0) exchange approximation the asymmetry for scattering to discrete states can be written as [27–30],

$$A_{RL}^{Res} = A_0 \frac{v_L R_{AV}^L(q, \omega) + v_T R_{AV}^T(q, \omega) + v_{T'} R_{VA}^{T'}(q, \omega)}{v_L R^L(q, \omega) + v_T R^T(q, \omega)}, \quad (3)$$

where L , T , and T' stand for longitudinal, transverse, and axial, and $v_{L,T}$'s are lepton kinematic factors. The term $A_0 \approx 6.5 \times 10^{-4}$ [28–30] and the subscripts AV and VA denote axial-vector leptonic and vector hadronic currents and vector leptonic and axial-vector hadronic currents. The parity violating responses $R_{AV}^{L,T}$ can be decomposed in terms of their isospin content [28–30],

$$R_{AV}^{L,T} = \beta^{I=0} R_{L,T}(I=0) + \beta^{I=1} R_{L,T}^N(I=1), \quad (4)$$

$$\beta^{I=0} = -2 \sin^2 \theta_W, \quad \beta^{I=1} = (1 - 2 \sin^2 \theta_W), \quad (5)$$

and I is the isospin quantum number. In the case of $N(1520)$, which is an isospin $\frac{1}{2}$ state, both terms in equation (5) contribute to the asymmetry. If one makes the approximation $\sin^2(\theta_w) = 0.25$ (so that the vector leptonic current, which multiplies the axial hadronic current, is zero), then in the limit of pure magnetic or electric scattering, and assuming isospin symmetry and negligible strange and charm form factors, the proton asymmetry can be written as:

$$A_{RL}^{Res,p} = -0.9 \times 10^{-4} Q^2 \frac{\sigma_n}{\sigma_p}, \quad (6)$$

a remarkably simple equation. For the deuteron, the result has a different sensitivity to nuclear structure and with these approximations becomes:

$$A_{RL}^{Res,d} = -0.9 \times 10^{-4} Q^2 R(W). \quad (7)$$

where $R(W)$ depends on the relative $I = 1$ compared to $I = 0$ strength, and is unity for a pure $I = 1$ transition, and is negative for a pure $I = 0$ transition.

We stress that these simplified relations are only presented here to bring out the main features of the PV asymmetry, and that the real structure is more complex (interplay of $I = 0$ and $I = 1$ and electric/magnetic or transverse/longitudinal strength) and the terms we are neglecting (axial current, strange and up/down sea quarks) are interesting and will be more fully addressed in the actual data analysis.

Although the formalism was worked out long ago [31], to the best of our knowledge the details have so far only been worked out for the case of elastic scattering [32] and the $N \rightarrow \Delta(1232)$ transition [9, 33, 34], although there is an ongoing effort to understand the higher W region [28–30], in particular the influence of meson exchange currents. An approximate model for the $S_{11}(1530)$ resonance was very recently presented in the Ph.D. thesis of Sacco [35].

A detailed prediction of the $N \rightarrow \Delta(1232)$ proton asymmetry is given by [33, 34] $A_p^\Delta = -[1.04 + 0.27F(Q^2, E, E', \theta_e)] \times 10^{-4} Q^2$ where $F(Q^2, E, E', \theta_e)$ contains the information on weak transition form factors, and is expected to be of order unity for $Q^2 < 1 \text{ GeV}^2$, decreasing to zero at very large E (or small $Q^2/2ME$) [32]. In the moderate Q^2 and energy of this proposal, this detailed prediction is within 20% of the simple model given by Eq. (6), since $\sigma_n/\sigma_p = 1$ for the isovector $\Delta(1232)$ resonance.

2. Deep-Inelastic Asymmetry

In the Standard Model and assuming quark degrees of freedom, the asymmetry arises from the interference between photon and Z exchange diagrams, and is given by [32]

$$A = \frac{\sigma_R - \sigma_L}{\sigma_R + \sigma_L} = -\frac{2Q^2}{M_Z^2} \frac{\sum f_i(x)(Q_i^\gamma/e)[g_A^e g_V^i + Y g_V^e g_A^i]}{\sum f_i(x)(Q_i^\gamma)^2}, \quad (8)$$

where $f_i(x)$ are the quark distribution functions for a quark of type i , Q_i^γ are the quark charges, the g 's are the electroweak axial and vector charges, $Q^2 = -q^2$ is the four-momentum transfer squared ($Q^2 > 0$ for our kinematics), M_Z is the mass of the Z boson, and

$$Y = \frac{1 - (1 - y)^2}{1 + (1 - y)^2 - y^2 R / (1 + R)} \quad (9)$$

where $y = \nu/E$, $\nu = E - E'$ is the energy lost by an incident electron of energy E scattering to an electron of energy E' , and the factor $R = \sigma_L/\sigma_T$ takes into account [36] the longitudinal contributions to both Z and photon exchange. Performing the sums and re-writing M_Z in terms of the α and G_F coupling constants, for a proton target we obtain

$$A_p = \frac{3G_F Q^2}{\pi\alpha 2\sqrt{2}} \frac{2C_{1u}[u(x) + c(x)] - C_{1d}[d(x) + s(x)] + Y[2C_{2u}u_v(x) - C_{2d}d_v(x)]}{4u(x) + d(x) + s(x) + 4c(x)}. \quad (10)$$

where the products of weak charges in the Standard Model at tree level are given by:

$$\begin{aligned} C_{1u} &= g_A^e g_V^u \\ C_{1d} &= g_A^e g_V^d \\ C_{2u} &= g_V^e g_A^u \\ C_{2d} &= g_V^e g_A^d. \end{aligned} \quad (11)$$

When Standard Model electroweak radiative corrections are included the C_{ij} become [37]

$$\begin{aligned} C_{1u} &= \rho' \left(-\frac{1}{2} + \frac{4}{3} \kappa' \sin^2(\theta_w) \right) + \lambda_{1u} \approx -0.1886 \\ C_{1d} &= \rho' \left(\frac{1}{2} - \frac{2}{3} \kappa' \sin^2(\theta_w) \right) + \lambda_{1d} \approx 0.3414 \\ C_{2u} &= \rho \left(-\frac{1}{2} + 2\kappa \sin^2(\theta_w) \right) + \lambda_{2u} \approx -0.0359 \\ C_{2d} &= \rho \left(\frac{1}{2} - 2\kappa \sin^2(\theta_w) \right) + \lambda_{2d} \approx 0.0265. \end{aligned} \quad (12)$$

In the limit of no electroweak radiative correction $\rho = \rho' = \kappa = \kappa' = 1$ and $\lambda_{1u} = \lambda_{1d} = \lambda_{2u} = \lambda_{2d} = 0$.

We have assumed that the $u(x)$, $d(x)$, $s(x)$, and $c(x)$ quark parton distribution functions (PDFs) of the proton can be described in terms of valence (v) and sea (s) contributions as

$$\begin{aligned} u(x) &= u_v(x) + u_s(x) + \bar{u}_s(x) \\ d(x) &= d_v(x) + d_s(x) + \bar{d}_s(x) \\ s(x) &= s_s(x) + \bar{s}_s(x) \\ c(x) &= c_s(x) + \bar{c}_s(x) \end{aligned} \quad (13)$$

The quark distribution functions depend mainly on the Bjorken scaling variable $x = Q^2/2M\nu$ (where M is the nucleon mass), but also evolve slowly with Q^2 due to QCD and finite mass corrections. While not shown explicitly, all quantities involving PDFs are functions of both x and Q^2 .

In the valence region, A_p is numerically approximated using Eq. (10) and Eq. (12), by

$$A_p = -10^{-4} Q^2 \frac{[0.51 + 0.45r(x) + 0.10Y(1 + r(x))]}{[1 + 0.25r(x)]}, \quad (14)$$

where Q^2 is in units of GeV^2 , $r(x) = d(x)/u(x)$, and we have ignored the strange and charm quark. Using isospin symmetry and with the approximation $\sin^2(\theta_w) = 0.25$, this can be written as

$$A_p = -0.9 \times 10^{-4} Q^2 \frac{2(1 + \sigma_n/\sigma_p)}{5}. \quad (15)$$

For the case of scattering from the deuteron, the full expression for the asymmetry is:

$$A_d = -10^{-4} Q^2 \frac{[0.78 + 0.41R_c(x) + 0.37R_s(x) + 0.10YR_v(x)]}{[1 + 0.2R_s(x) + 0.8R_c(x)]}, \quad (16)$$

where $R_c(x) = 2c(x)/[u(x) + d(x)]$, $R_s(x) = 2s(x)/[u(x) + d(x)]$, and $R_v(x) = [u_v(x) + d_v(x)]/[u(x) + d(x)]$. This equation can be simplified in the valence region using $\sin^2(\theta_w) = 0.25$ to yield

$$A_d = -0.7 \times 10^{-4} Q^2, \quad (17)$$

which is about 20% less than the simplified transition form factor model for a pure $I = 1$ transition.

The main goal of JLab E05-007 (DIS-parity) is to measure a linear combination of C_{2u} and C_{2d} using a deuteron target in a kinematic region where the partonic picture is expected to be valid. Deviations from the Standard Model values could be a sign of new physics. In the kinematic region of the present proposal (low Q^2 and W), we expect deviations from the Standard Model to occur principally from coherent resonant effects (higher twist effects in the language of the QCD), which should die away at higher Q^2 .

B. Physics of the Proton Measurements

Much of our knowledge of resonance structure for the proton comes from unpolarized measurements in the resonance region, both for inclusive and exclusive processes. Measurements of the parity violating response provide additional information on the resonance structure of the proton, while allowing first investigations of duality and higher twist contributions to the parity violating asymmetry in the proton.

1. Parity Violating Response in the Resonance Region

Recent measurements of the separated structure functions [3] and polarized structure functions [4] have provided new information on the resonance region, such as larger than expected longitudinal strength in the region of the Δ and unexpectedly large strength in the longitudinal (F_L) and polarized (A_1) structure functions in the vicinity of 1385 MeV [3, 38]. Measurements of the parity violating response can provide further information on the proton resonance structure. Because of the much different isospin structure and different couplings, the weak current will couple to individual resonances differently than the electromagnetic current, which can help in identifying new or poorly established resonances.

At the moment, there are no measurements of the parity violating response in the resonance region, and the only planned measurement is for the $N \rightarrow \Delta$ transition at large scattering angle and low Q^2 [39]. Calculations exist only for the elastic response and the $N \rightarrow \Delta$ transition; there are no explicit calculations for the higher resonances.

The dashed curve in Fig. 2 shows a predicted asymmetry for the proton calculated with the simplified model of Eq. (6) at the average Q^2 of this proposal. Because there are no empirical models that describe σ_n/σ_p in the resonance region for a free neutron, we made a rough guess using a resonance region fit to σ_p divided by a DIS fit to σ_p , normalized to unity at the peak of the $\Delta(1232)$ resonance. While this fit may have little to do with reality (except at the Δ peak), it does give an idea of the approximate size and width of the likely oscillations around the full DIS prediction of the asymmetry (Eq. 10 with a standard set of PDFs), shown as the solid curve. Once the results of the BONUS experiment in Hall B are analyzed, it will be possible to have a much more realistic prediction for the free neutron to proton cross section ratio. In any case, it is clear that the predictions shown in Fig. 2 are of similar magnitude, when averaged over resonance structure. This may be a manifestation of quark-hadron duality, as discussed in the next section.

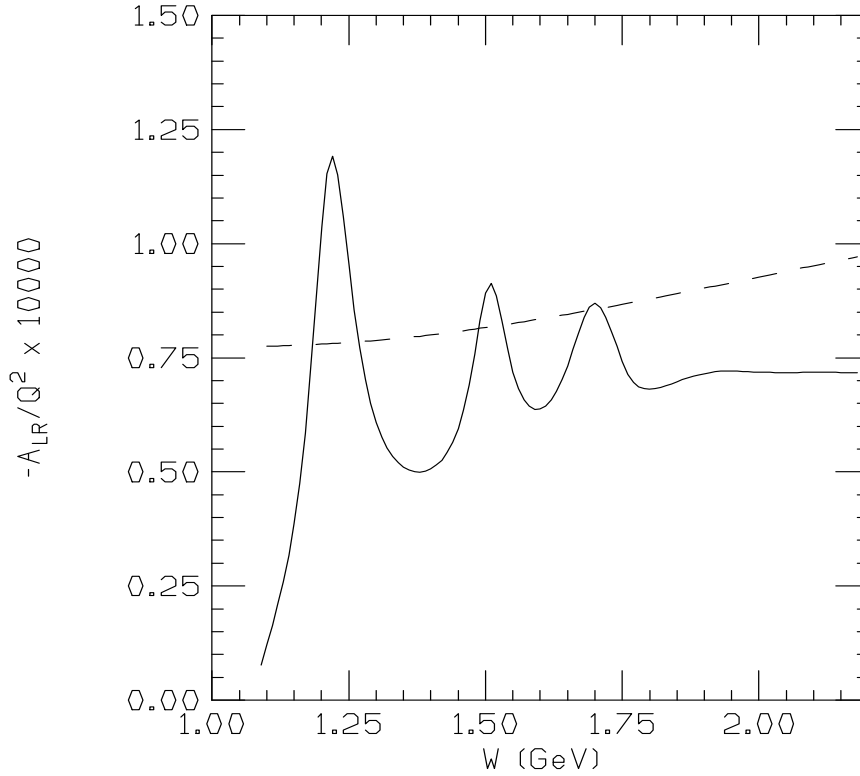


FIG. 2: Full DIS prediction (solid curve) and simplified resonance region prediction (dashed curve) for the normalized proton asymmetry at the average $Q^2 = 0.8 \text{ GeV}^2$ of this proposal.

2. Duality

Quark-hadron duality was first observed by Bloom and Gilman in 1970 [6]. It postulates that physical quantities calculated in the hadronic description give the same results as if they were calculated using the partonic description if a proper scaling variable that connects the two kinematic regions is used. In QCD, De Rujula, Georgi and Politzer [5] have shown that duality can be understood from an operator product expansion of moments of structure functions, which allows one to separate the short and long distance contributions to the moments of structure functions. The leading terms in the OPE correspond to scattering from free quarks, which are responsible for scaling, while higher terms take interactions between quarks and gluons (higher-twists) into account. In the resonance region if the higher-twists are not significant then the moments of structure functions cannot be much different than the corresponding scaling value, which is given by the moments of the leading-twist term. Therefore, if a structure function rises above the scaling value it has to fall in the neighboring region (or oscillate around the scaling function) in order to compensate for the increase or decrease in the moments above the scaling value. This explains why resonances average to a smooth scaling curve. This behavior observed over restricted regions in W for each resonance is known as local duality. So far duality has been seen to work for unpolarized structure functions for the electromagnetic tensor, W_1^{EM} and W_2^{EM} , to Q^2 as low as 0.5 GeV^2 [3, 8, 40]. Figure 3 shows the structure function νW_2^{EM} as a function of the Nachtmann scaling variable, $\xi = 2x/[1 + \sqrt{1 + 4x^2 M_N^2/Q^2}]$, for different Q^2 values. The data clearly demonstrate that duality works remarkably well to rather low values of Q^2 .

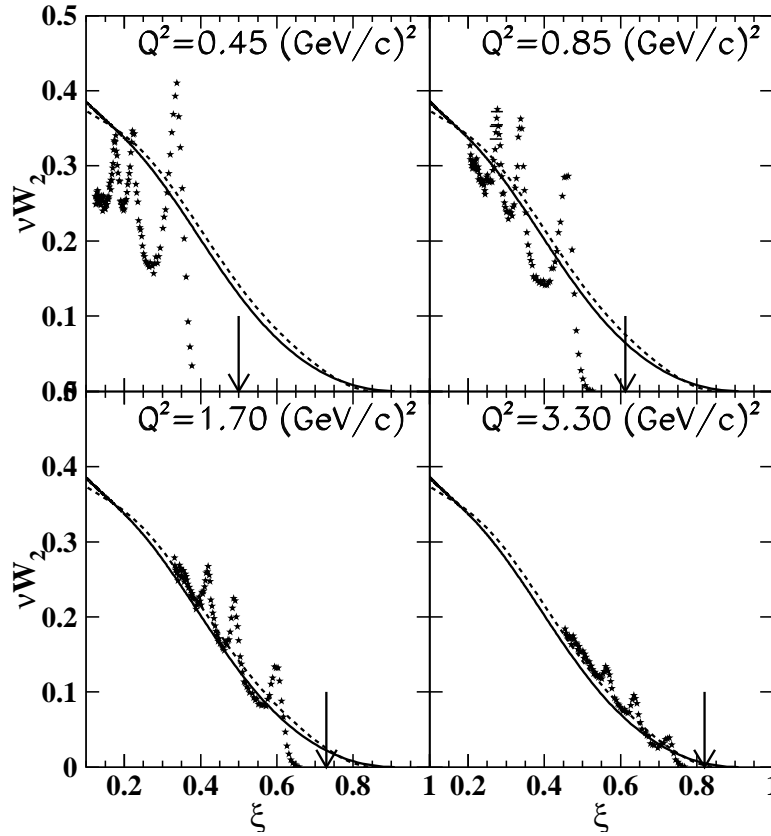


FIG. 3: The spin independent structure function νW_2^{EM} plotted as a function of $\xi = 2x/[1 + \sqrt{1 + 4x^2 M_N^2/Q^2}]$ for hydrogen at different Q^2 values [40]. The solid and dashed lines are a fit to deep inelastic structure function data at $Q^2 = 10 \text{ (GeV/c}^2\text{)}$ and $Q^2 = 5 \text{ (GeV/c}^2\text{)}$ respectively. The arrows correspond to the inelastic threshold.

In terms of structure functions, to lowest order in the weak and electromagnetic currents, A_{RL} can

be written as,

$$A_{RL} = \frac{Q^2}{Q^2 + M_Z^2} \frac{g_A (2W_1 Q^2 + W_2 (4EE' - Q^2)) - g_v W_3 Q^2 (E + E')/M}{2W_1^{EM} Q^2 + W_2^{EM} (4EE' - Q^2)}, \quad (18)$$

where $W_{1,2,3}$ are structure functions for the interference tensor of the electromagnetic and weak neutral hadronic currents, g_v and g_A are the vector and axial-vector coupling constants at the lepton- Z^0 vertex and E and E' are the energies of the incoming and outgoing electron. The denominator of the asymmetry A_{RL} depends only on W_1^{EM} and W_2^{EM} . Both of these structure functions are very well measured and understood at the Q^2 values of this experiment and can be determined using a model. Although it is not possible to separate the structure functions for the interference tensor, A_{RL} can be used to test duality for a linear combination of W_1 , W_2 and W_3 (numerator of Eq. (18)). Duality has never been tested for these structure functions to date. As pointed out in the previous section, the interference cross section is expected to show a resonance structure that depends on the isospin of the final excited state.

Essentially, the leading order criteria for duality to work can be written as

$$(\sigma_n/\sigma_p)^{res} = \frac{2}{5} (1 + (\sigma_n/\sigma_p)^{DIS}) \quad (19)$$

The two different dependencies on σ_n/σ_p come from the fact that in the resonant case, the current is expressed through the square of the sum over parton charges, while in the DIS limit, it is the sum of the squares which gives the current. As pointed out by Close and Isgur [10], the cross terms can cancel on average when opposite parity states are mixed. Fig. 2 also indicates that the average of the $\Delta(1232)$ and the elastic peak region tend to equal the DIS curve, and that at higher masses there are many resonances whose sum may oscillate around a value of the same order of magnitude as the DIS limit. We note that Eq. (19) is satisfied if on average $\sigma_n/\sigma_p = 2/3$, which is perhaps not a bad approximation.

This simple model gives us an indication that duality in the weak neutral current might be valid, to some extent, in a leading order valence picture of the vector hadronic current. Only with actual data can we determine the extent to which duality works or fails. What is of particular interest is to study the deviations due to the different mixture of resonances, their isospin structure, and their axial form factors.

In fact, a recent calculation for the $N \rightarrow \Delta$ transition predicts that the deviation from duality will be much larger for the PV asymmetry than in either the polarized or unpolarized structure functions [9]. The predictions are based on a dynamical model of pion electroproduction [41, 42], which has been extended to include the neutral current contributions through weak pion production reactions [43]. To evaluate the contributions to the asymmetry A_{RL} from the three structure functions $W_{1,2,3}$ the following simplified form of the asymmetry is used;

$$A_{RL} = 8.99 \times 10^{-5} Q^2 (1.075 + \Delta_V + \Delta_A). \quad (20)$$

The term Δ_A depends on W_3 that can only have the contributions from the axial vector parts of the neutral currents and the term Δ_V depends on $W_{1,2}$ that can only have contributions from the vector parts of the neutral current. The calculations show that Δ_V is weaker than Δ_A near the Δ resonance. Therefore, the asymmetry data at the $\Delta(1232)$ can also be used to extract the contributions from the axial vector currents. Fig. (4) shows the asymmetry of $p(\vec{e}, e')$ predicted by the model (solid curves) for two incident electron energies. These calculations predict a 50% deviation from duality predictions (i.e. calculations based on the parton model) in the Δ region for our kinematics. Further, the authors point out [44] that a 20% change in $f_{\pi NN}$ or $f_{\pi N\Delta}$ yields a change in the asymmetry of <1% for the Δ region (for $0.1 < Q^2 < 1 \text{ GeV}^2$), while a 20% change in g_A for NN ($N\Delta$) yields a change of <0.5% (2%) for the same kinematics. It is important to point out that the model calculation does not include non-resonant background. However, this should be small for the Δ region at the proposed Q^2 values. This model predicts duality for unpolarized cross sections and small deviations from duality for the spin-dependent structure functions, in fairly good agreement with both polarized and unpolarized data.

In the case of the deuteron, the simplified formulas Eq. (7) and Eq. (17) differ by 20% for $R(W) = 1$ (as for the $N \rightarrow \Delta$ transition in the absence of non-resonant background terms). On the other hand, the average of the quasi-elastic and $\Delta(1232)$ asymmetries lies close to the DIS prediction.

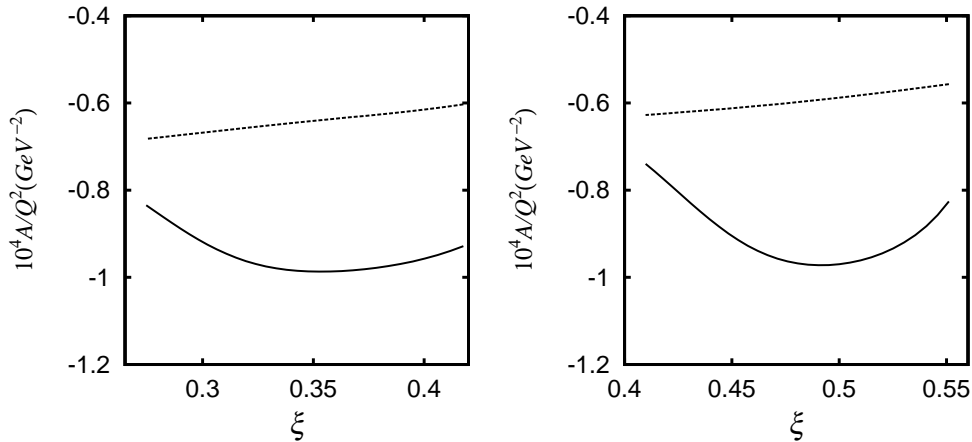


FIG. 4: The asymmetry of $p(\vec{e}, e')$ predicted by the extended Sato-Lee model (solid curves) as a function of the Nachtmann scaling variable ξ for the incident electron energy $E = 4$ GeV (left) and $E=6$ GeV (right). The model calculations are compared with the parton model predictions calculated using the CTEQ6 parton distribution functions (dashed curves).

Only with experimental data (which will include the effects of the axial current, strange form factors and higher twist contributions) will we be able to test how well duality works. We can test duality locally to better than 5%, and globally down to 2–3%, comparable to the limits on duality in the unpolarized F_2 structure function. A quantitative understanding of duality in PV electron scattering will provide new constraints for models trying to understand duality and its QCD origins. In addition, if duality is observed to hold at the few percent level at the lower W^2 and Q^2 values of this measurement, it would provide significant limits on the contributions of higher twists to 12 GeV measurements in the DIS region, designed to look for physics beyond the Standard Model, the $d(x)/u(x)$ ratio at large x , and strange quark distributions.

C. Nuclear Targets

We will also take data on carbon and deuterium targets covering the same kinematics as the hydrogen data. This will allow studies of duality and higher twist in these nuclear targets, as well additional studies related to the nuclear dependence of the parity violating response. This will be important for future parity violating measurements in the DIS regime, as well as measurements of neutrino scattering which are performed on nuclear targets.

Isospin separation with unpolarized electrons relies on the use of neutrons embedded in nuclei such as deuterium, in which the effects of Fermi motion and Pauli suppression must be taken into account. On the other hand PV electron scattering on the proton allows access to a new isospin combination free from these effects, just as measurements on the proton in the DIS region can extract the ratio $d(x)/u(x)$, free from nuclear effects.

1. Duality and Higher Twist

In unpolarized scattering from deuterium, the structure due to individual resonances can be seen at low Q^2 values, although it is broadened due to Fermi motion. We may observe similar structure in the parity violating asymmetry, in which case deuterium data can be combined with proton data to study neutron resonance structure. However, we do not know in advance how strong the contribution of individual resonances to the asymmetry will be, and so we do not know for certain if we will be able to extract information on individual resonances.

Even if we do not see large contributions from individual resonances, we can still study duality in deuterium and carbon. While Fermi broadening makes it difficult to study duality resonance-by-resonance in the deuteron, measurements of scaling and duality in nuclei [8, 45–47] have shown that duality is also valid in nuclei, while analyses of the lowest moments for nuclei are consistent with perturbative evolution down to $Q^2 \lesssim 1 \text{ GeV}^2$ [48, 49]. We will be able to test duality in the parity violating asymmetry for nuclei at a level comparable to the unpolarized structure functions. If duality holds as well as it does for F_2 , we will be able to set limits on higher twist contributions that will be significant for future parity violation measurements at Jefferson Lab.

There are no measurements of the higher twist contributions to the parity violating asymmetry. Calculations have been made for the $e^{-2}H$ asymmetry, yielding contributions of order one percent for $Q^2 \approx 1 \text{ GeV}^2$ [50, 51]. Phenomenological estimates were made for the DIS-parity proposal [52], based on the higher twist analysis [53] of high precision data on F_2 for hydrogen and deuterium. These estimates also predict HT contributions at the $1\%/Q^2$ level. While a 1% correction for DIS-parity would be small enough that it would not impact the interpretation of their data, it is important to make measurements that can directly constrain the HT terms in the asymmetry.

The approved DIS-parity measurement will extract HT contributions with an uncertainty at the level of $3.5\%/Q^2$ for deuterium at $x \approx 0.3$; the first experimental limit on HT for PV scattering. The proposed measurement would set improved limits ($2\%/Q^2$) on higher twist terms for deuterium, and will allow measurements over a range in x of $0.2 \lesssim x \lesssim 0.6$. We will obtain similar measurements for carbon, and slightly worse ($3\%/Q^2$) for hydrogen, both over the full x range.

Note that these data can also be used to constrain higher twist corrections in the NuTeV determination of $\sin^2(\theta_w)$. Models can be used to connect the HT corrections to PVES to those for the NuTeV measurements. Using this approach, Gluck and Reya [54] showed that the HT contributions for the NuTeV measurement at large Q^2 ($\approx 20 \text{ GeV}^2$) can be related to the PVES HT corrections for $Q^2 \approx 2 \text{ GeV}^2$. A 2.5% HT contribution would be enough to resolve the $\approx 3\sigma$ NuTeV anomaly, and the corresponding higher twist corrections to our proposed measurements on deuterium and carbon could be large enough to be measurable (because of the lower Q^2 of our proposal).

2. EMC ratios

We can also use these data to study the nuclear dependence of the parity violating asymmetry. The PV asymmetry provides a probe with very different sensitivities to the usual EMC ratios from unpolarized scattering. If the EMC effect is the result of a uniform modification of all quark (and anti-quark) distributions, then it will have an identical effect on both the photon and Z exchange, yielding no EMC effect for the asymmetry. Thus, any observed medium modification would have to come from something beyond a simple rescaling of quark distributions - either a flavor dependence to the EMC effect, a difference between the modification of valence and sea contributions, or an additional nuclear dependence related to Z exchange.

We know little about the isovector contribution to the EMC effect, and nothing about nuclear dependence in Z exchange. If we measure a significant effect, it will be very interesting physics, although this measurement itself will not be able to definitively determine the origin. The proposed measurements will only study carbon and are limited by statistical accuracy. If such a nuclear effect is observed, one could make higher precision measurements and include heavier targets to better constrain the effect. This could be combined with measurements on nuclear targets from MINERvA or other neutrino scattering measurements to better understand the origin of the nuclear effects.

While the proposed measurements are in the resonance region, this is precisely the region that dominates interactions in many of the high precision neutrino measurements, thus making nuclear effects in this region important, even if they cannot be trivially connected to nuclear quark distributions. In addition, nuclear dependence of the unpolarized structure function shows identical behavior in the DIS and resonance region, down to very low W^2 values [47]. Recent work showing a very different EMC effect for spin structure functions [55, 56], with a noticeable difference in the effect on the up and down quark distributions [55], makes such a measurement all the more appealing. Thus, the observation of a significant nuclear dependence in PVES would be of great interest, while setting meaningful limits

on such dependence would be useful for other neutrino scattering or PVES measurements on nuclear targets.

D. Impact on other measurements

The proposed measurements will provide interesting new information on the parity violating response of the resonances, duality in the PV asymmetry, and nuclear dependence of the PV response. In addition, they will be relevant for other important parity measurements, some already proposed and others planned for the 12 GeV upgrade. Such high precision measurements can provide a great deal of information on the structure of the nucleon as well as providing important tests of the standard model. However, it is very difficult to make sure high precision measurements at isolated kinematic points, without a good understanding of the parity violating response over a broad range of (x, Q^2) . Measurements of PVES in the resonance region provide input to understand backgrounds, radiative corrections, and higher twist effects in these very important measurements. In some cases, these data will have a direct impact on future measurements, by providing direct measurements of backgrounds and improving global models of the PV response needed for radiative corrections. In other cases, these data will give an indication of where additional measurements of backgrounds or higher twist contributions will be critical for the success of these measurements.

Knowledge of higher twist contributions, which can be large but are very difficult to estimate, is extremely important for the planned DIS parity violation measurements at 6 and 12 GeV. The approved DIS-parity measurement on deuterium (their Phase I measurement) will extract HT contributions to their high Q^2 measurement with an uncertainty of $\approx 2\%$, while Phase II, if approved, is expected to reduce this to 1.5%. Our proposed deuterium measurement would yield a 1% uncertainty for their high Q^2 measurement, a factor of two improvement over their Phase I measurement, and a significant improvement over the planned Phase II measurements.

In addition to improving on the DIS-parity limit on deuterium at $x \approx 0.3$, we will provide comparable constraints for hydrogen, deuterium, and carbon over a significant range in x . This will be important for some of the parity measurements proposed at 12 GeV which aim to extract $d(x)/u(x)$ with measurements on the proton to avoid the large uncertainties associated with nuclear effects. This data will extend to larger x than the 6 GeV measurements, where higher twist contributions will be a larger concern. This initial measurement will give important information about size of HT contributions as a function of x , which will help in determining the regions where 12 GeV measurements are likely to be free from significant HT contributions, and regions where further work will be necessary to determine that HT contributions are sufficiently small.

Another benefit of the proposed measurements is improved understanding of backgrounds in other PV experiments. In the recently completed E158 experiment [57] at SLAC, the primary electron-electron (Møller) scattering signal was mixed with electron-proton scattering background, enhanced through radiative effects by the relatively long 180 cm LH2 target. While the ep elastic contributions are relatively well understood, the inelastic contribution (with an asymmetry about 20 times larger than the Møller asymmetry), turned out to generate the largest correction to the measured asymmetry and yields the largest systematic error of this experiment (22 ppb, or 17% relative). Direct measurements of the W dependence of PV inelastic scattering will help to build confidence in the systematic error on the E158 result, which is at present one of the three most precise Standard Model tests away from the Z pole, and will also be of value for future Møller PV experiments, for example with JLab at 12 GeV. The background issues will be different for a 12 GeV Møller measurement, and the details will depend on the final detector designed for such a measurement. However, the goal is to make a measurement that is roughly a factor or four times more precise than the E158, meaning that it will be crucial to have a significantly better control over the corrections, through a combination of experiment design aimed at reducing the background, and improved knowledge of the background asymmetries. The measurements proposed here can provide important input to such a future measurement, both as a direct measurement of the asymmetries for some of the background processes, and by providing input to help guide the design of the experiment and/or any additional dedicated measurements needed to reach the desired precision.

Finally, the proposed measurements will be an essential input to calculations of radiative corrections

to measurements in the DIS region. The present lack of knowledge of asymmetries in the resonance region introduces significant errors in the contributions to DIS electron scattering, and in particular the already approved DIS-parity experiment (for which W is only slightly above the resonance region). For a precision Standard Model test with 11 GeV electrons, we estimate the present uncertainty in radiative corrections from the resonance region asymmetries will correspond to as much as a 1.5% error in the DIS asymmetry, which would be the largest systematic error of the experiment. This measurements of this proposal will reduce this error to $< 0.3\%$.

III. EXPERIMENT

The primary goal of the experiment is to measure A_p , A_d , and A_C in and slightly beyond the traditional nucleon resonance region ($M < W < 2.1$ GeV) at moderate Q^2 . The choice of hydrogen and deuterium as the targets is dictated by the desire to observe possible resonance structure, without the large blurring effects of Fermi motion and shadowing in heavier nuclei, and to test duality using the weak neutral current with two isospin combinations, for which the predictions are quite different, as was discussed above. Measurements with both hydrogen and deuterium have a further advantage, in that the ratio of asymmetries is almost free of experimental systematic errors, allowing a very precise comparison with theory. The data on carbon allows a first look at the nuclear dependence in PV electron scattering, while also providing input for cross section models needed in precise neutrino scattering measurements and backgrounds for other PV electron scattering measurements.

The minimum useful Q^2 is limited to about 0.5 GeV² due to increasingly large elastic radiative tails at low Q^2 (which dilute the measured asymmetry), and by the smallest practical scattering angle for a large solid angle spectrometer. The maximum Q^2 is limited to approximately 1 GeV² by the beam energy and the rapidly decreasing cross sections with increasing Q^2 . The range of $0.5 < Q^2 < 1$ is well matched to that where the onset of duality is seen to occur in the spin-averaged proton response functions, as well as the spin-dependent structure function g_1 [8]. We have picked an average Q^2 of 0.8 GeV² as giving the best sensitivity to the physics issues we wish to study.

The experimental asymmetry is diluted by the beam polarization P_e , so that

$$A_{exp} = \frac{N_+ - N_-}{N_+ + N_-} = P_e A,$$

where N_+ and N_- are the number of scattered electrons detected from $+$ and $-$ beam helicities respectively. The statistical uncertainty is given by

$$\delta A = \frac{1}{P_e \sqrt{N_+ + N_-}}.$$

For Q^2 in the 1 GeV² range, on the order of 10^{12} electrons must be detected to achieve a 1% uncertainty in the physics asymmetry.

For $Q^2 = 1$ GeV², typical asymmetries are of order 100 ppm, large compared to the typically few ppm asymmetries of HAPPEX or G0 experiments at JLab, and comparable to the raw asymmetries measured in Hall B with polarized electrons incident on polarized deuterons in ND3. This makes the requirements on beam systematics for this proposal (charge and position asymmetries and jitter, leakage from other Halls, etc.) considerably more relaxed than in previous PV experiments at JLab.

A. Optimization of Kinematics

Several considerations enter into the optimization of beam energy and spectrometer angle. The beam energy E must be at least 3 GeV to span the full resonance region. In practice, a higher beam energy of 4 GeV is needed to avoid large radiative tails at high W . For a given choice of Q^2 , the figure of merit (FOM) improves approximately linearly with E , due to the larger cross section at the correspondingly smaller angles. However, the maximum momenta of the HRS spectrometers (3.2 and 4.3 GeV) limits the

useful beam energy to 5.1 GeV. If we lower this to 4.8, we can take two settings with each spectrometer and have overlap between the higher and lower W settings. The best figure of merit is then obtained by running at the smallest possible angle that doesn't require the septum magnets, which is 12.5 degrees.

B. Beam Line and Polarimetry

We propose to use 4.8 GeV polarized beam with 80% polarization and 85 μA beam current. To reduce the heat impact on the target, the beam is circularly rastered such that the beam spot size at the target is ≈ 4 mm in diameter (or rectangularly rastered to a 4×4 mm² spot). The beam energy can be measured to a $\Delta E/E = 2 \times 10^{-4}$ level using either ARC or eP devices [58]. The beam polarization will be measured by the Compton polarimeter utilizing an upgraded (green) laser. Compton-scattered electrons and photons are detected by two sets of detectors and the data can be analyzed either inclusively or in coincidence. The systematic error of “electron only” method for a 4.8 GeV beam is 1.1%. Within 40 minutes of 85 μA beam the statistical error is 0.6%, giving a total error of 1.2%. The systematic error of “photon integration” method currently being developed by the HAPPEX collaboration is also expected to achieve a 1% level, providing a cross check of the electron method. The green laser upgrade of the Compton is already underway. It is expected to be installed in the hall in 2006 and will be used for two approved experiments PREX [59] and DIS-parity [52].

C. Parity DAQ (Hall A)

The parity DAQ in Hall A [60] and the beam helicity feedback system have been successfully used to control the beam helicity-dependent asymmetry for the Hall A parity experiments in the past. The asymmetry in the integrated beam current measured by the parity DAQ is sent to the polarized electron source where the Pockel cell voltage is adjusted accordingly to minimize the beam intensity asymmetry. Using this method the beam helicity asymmetry was controlled to the 10^{-7} level during HAPPEX. Since our measured asymmetry is much larger than that measured by HAPPEX, we request that the beam helicity asymmetry be controlled below 10^{-6} which will require only modest effort.

D. The Liquid Target

We choose to use two racetrack-shaped 25 cm long cells with 5 mil aluminum for both entrance and exit windows. This is the same cell design as needed for the DIS-parity proposal [52]. One cell will be filled by LD2 and the other by LH2. A 2.5 g/cm² carbon target (6% radiation length) will be added to the target ladder.

The target will be almost identical to the one used by HAPPEX in 2004-5, aside from the additional cell. The racetrack-shape is chosen because of its much smaller boiling effect than the commonly used cigar-shape (cylindrical) cells. Boiling tests on a LD2 cell will be performed during commissioning to optimize the running conditions. We plan to start from a 4×4 mm² raster and 60 Hz fan speed and the boiling noise will be measured up to a beam current of 90 μA . Such a test is also a pre-requisite for the approved DIS-parity experiment.

Boiling tests on racetrack-shaped LH2 cells were performed by the HAPPEX collaboration in 2004 [61], where a negligible boiling noise (< 100 ppm) was found for a 20-cm long LH2 cell and a 70 μA beam. A 5×5 mm² raster and 60 Hz fan speed were used for the test. The boiling noise of a LD2 cell is expected to be at the same level, and will not be a problem for the proposed measurement. Scaling the HAPPEX results to the slightly higher current, longer target, and smaller raster proposed here indicates that the noise should be < 250 ppm, a factor of 2–3 larger than for HAPPEX, compared to a physics asymmetry approximately 50 times larger. The highest rate for Res-Parity is 1.3 MHz, which for a 33 ms helicity pulse implies a yield of 43k events, yielding statistical fluctuations of $1/\sqrt{(43k)} = 0.005$. Additional fluctuations of ~ 250 ppm will yield a negligible broadening (a relative increase of 0.25%), and thus will not impact the uncertainty of the measurement.

We note that the experiment could also be done with the existing 20 cm HAPPEX cell, if need be, with some loss of luminosity (depending on how much higher beam current is available), some additional time to change from LH2 to LD2, and a possible increase in the systematic error on the ratio of proton to deuteron asymmetries.

E. Luminosity Monitor

The luminosity monitor (Lumi) in Hall A was successfully used for the HAPPEX experiment in their 2004 and 2005 run, and will be used for the two approved experiments PREX and DIS-parity. In the following we discuss how well the noise level can be controlled by the Lumi.

The Lumi consists of 8 pieces of quartz at 0.5° . Each piece has $2 \times 5 \text{ cm}^2$ effective area at 7 m from target. The rate for 4.8 GeV beam is $> 10^{11}$ Hz per piece. With this high rate, the false asymmetry and the target boiling effect have been monitored to a level of 100 ppm per pulse during the 2004 running of HAPPEX II for a $70 \mu\text{A}$ current and a $5 \times 5 \text{ mm}$ raster. With a $85 \mu\text{A}$ current and a $4 \times 4 \text{ mm}$ raster being proposed here, the noise level is expected to be controlled below the 10^3 ppm level and thus will add negligible effect to the statistical width of the measured asymmetry (0.01 per pulse).

Most of the events in the Lumi monitor are from elastic scattering. The asymmetry is in general proportional to Q^2 , hence the physics asymmetry detected by the Lumi is very small, of the order of < 100 ppb. Therefore the false asymmetry can be monitored to ≈ 100 ppb. Compared to the physics asymmetry that we propose to measure ($50 \sim 100$ ppm), this will cause a $< 0.2\%$ systematic uncertainty and is therefore negligible.

F. Spectrometers and Pole-tip Background

We use the standard Hall A High Resolution Spectrometer (HRS) to detect the scattered electrons. For each HRS the effective solid angle acceptance for an extended target is 6 msr and the momentum bite is $\pm 4.5\%$. The central momentum of the HRS can be calculated from the dipole field magnitude at the 5×10^{-4} level [58]. The HRS central angle can be determined to ± 0.2 mrad with careful analysis [62].

One of the concerns of most parity experiments utilizing spectrometers is the Møller-scattered electrons off the magnetized iron inside the spectrometer magnet (“pole-tip” background). This should be an extremely small effect for these measurements. Based on observed pole-tip scattering in previous measurements, we expect $< 3\%$ of the detected events to come from re-scattering, and simulations show that less than 10% of those involve scattering from magnetized iron. These scattered electrons are typically at much lower energy than the electrons of interest, and the calorimeter cuts in the counting electronics should reject $> 99\%$ of these events, yielding a contamination from events re-scattering from magnetized iron to be $< 0.003\%$. Taking into account the average electron polarization in the iron ($\sim 8\%$), the average electron polarization ($\sim 10\%$ after spin precession), and the analyzing power ($\sim 10\%$), we expect an asymmetry of $\sim 10^{-3}$ for these events. This is roughly a factor of ten larger than the physics asymmetry we are trying to measure, but since this background is $< 0.003\%$ of the rate of good events, we expect this correction to be negligible, being less than one-thirtieth of a percent on the measured asymmetry.

In addition, this background has been studied extensively by the HAPPEX collaboration. During their test runs, the angle of one spectrometer was set slightly away from the elastic peak such that elastically scattered electrons may hit the pole-tips. Such events are then tagged by the elastically scattered protons in the other spectrometer. Using this method an upper limit on the asymmetry from pole-tip events was found to be $\delta A < 10^{-8}$ [63]. Simulations were also performed to confirm this test result and in fact, the background asymmetry was found to be less than 2×10^{-9} in the simulation [63]. We scale the HAPPEX number by the ratio of electron flux, detector acceptance, also consider that not all pole-tip events can survive the event selection of the DAQ, and find the pole-tip background for the proposed measurement to be $\delta A < 7 \times 10^{-8}$. Compared to the $50 \sim 100$ ppm physics asymmetry of this proposal, the pole-tip contribution is $< 0.02\%$.

G. Particle Identification Detectors

Particle identification (PID) in each HRS will be done with a CO₂ Cherenkov detector and a double-layered lead glass shower detector. Based on data from past experiments, the combined pion rejection factor of these two detectors was found to be $\geq 10^4$ [64] for a given electron efficiency of $\geq 99\%$ each. At high rate, a practical estimate of the PID efficiency should also take into account the effect of event pileup, detector readout deadtime and electronic noise. We simulated these effects and the pion rejection with the fast counting DAQ is expected to be better than 10^3 .

H. Fast Counting DAQ

To separate the pion background we will use a counting method. The counting method has been used successfully at 100 MHz by the Mainz A4 parity violation experiment [65, 66]. Also relevant is the experience of the G0 collaboration in deploying a counting method [67]. We plan to use a Flash ADC (FADC)-based fast counting DAQ which has virtually no deadtime, and use a scaler-based DAQ as cross check. This strategy will also be used for the DIS-parity experiment and test runs of both DAQs using a small fraction of the PID detectors are already underway by the DIS-parity collaboration. The basic principle of these two DAQs is described in the following section. In addition, we will take low rate runs to provide a sample of events with full tracking and particle identification information, as a further systematic check.

1. FADC-based DAQ

The detector signals we will use include the 10 PMT signals from the gas Cherenkov detector and the approximately 180 signals from two layers of lead glass detectors. To reduce the processing time and the noise, as well as the number of FADC modules, both detectors will be segmented. PMT signals from each segment are first summed and then sent to the FADC for digitizing. Segmentation of the detectors will also allow binning in W and Q^2 , the central value of which can be checked by taking data with regular HRS DAQ at low rates. In addition, the 24 signals from scintillators might be useful for crude directional information.

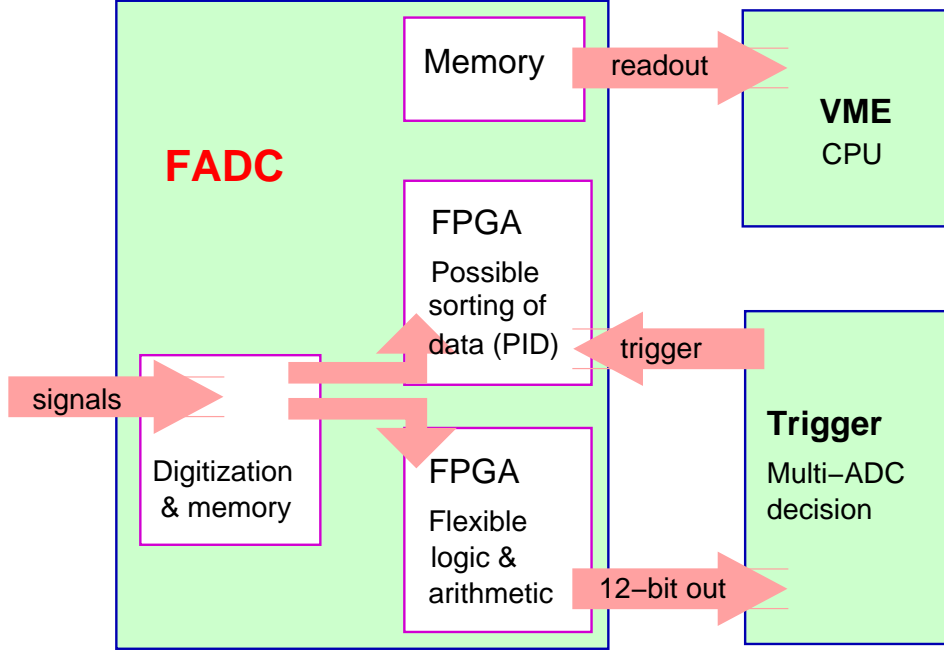
For the FADC we are considering a modified version of the one presently being designed by the Fast Electronics Group at JLab. A schematic diagram is given in Fig. 5. This FADC design will allow for the possibility of counting experiments at approximately 1 MHz with virtually no deadtime. The FADC fills an on-board memory at 250 MHz with $\approx 8 \mu\text{sec}$ latency (buffer size), recording both amplitude and timing information about the signal. An on-board processor (FPGA) will analyze the digitized data, with intermediate results sent to an external trigger processor to form a trigger based on multiple FADC boards. The trigger capability is not needed for the present proposal, but if available can be used to fully sample a subset of the data (TDC and ADC information). The scheme will be flexible enough to accommodate a variety of experiments. Parasitic tests were made of HRS detector signals using a 100 MHz Flash ADC in mid-2005, and these results were used to make a detailed design specification for the FPGA [68]. A first version of the FADC should be ready sometime in 2007.

The on-board algorithm shall permit an online identification of electrons, pions, and associated pileup, and counts these in local memory on the FADC. The data which is read out from the FADCs by the VME cpu is the number of these particles integrated over the helicity pulse, usually at 30 Hz, and possibly at a higher sampling rate, say 600 Hz. In a test mode the entire FADC data may be read (at the price of some deadtime) to check the reliability of the algorithm.

Electrons are identified as events which pass the Cherenkov cut and which deposit a sufficient total energy in the lead glass, while pions leave no signal in the Cherenkov and small average signals in the lead glass. The efficiency of the cuts and the cross contamination of the particle samples can be checked at very low beam current. From experience in Hall A, these efficiencies and contaminations are already known under running conditions similar to the proposal. Pileup of two particles will occur

FIG. 5: Schematic diagram for the fast DAQ system (a possible 2nd generation of JLab in-house design).

250 MHz, 8 usec latency, 1 MHz on-board analysis, 0.1% DT measurement



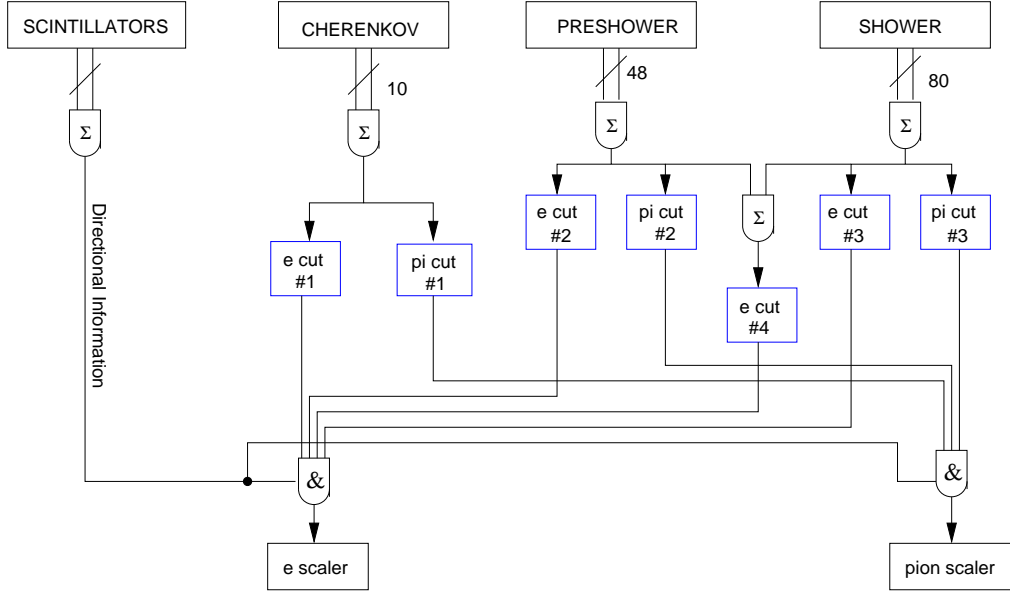
in approximately 6% of events if we make no changes to the existing phototubes which have a 60 nsec resolving time. Although these effects are not easy to study directly at high rates, we can indirectly study them by an analysis in which the data of independent events are added. The pileup effects include: 1) $e^- - e^-$; 2) $e^- - \pi$; 3) $\pi - \pi$. Since electrons must only pass a threshold, electrons accompanied by a secondary particle will still be counted as electrons; however, a correction must be applied for two-electron pileup. These can be measured using a higher threshold cut on the lead glass and counting the events that pass this higher threshold. For the lowest momentum setting of the proposed measurement where the π/e ratio is the highest, a total rate of 1.3 MHz (800kHz e^- and 500kHz π^-), the pileup involving pions will result in a (1.5–2.0)% loss of the pion count rate, since they tend to be moved away from the one-pion cut window. A fraction (0.5–1)% of two pion events will be counted erroneously as electrons. These effects from pions can be corrected with sufficient accuracy and the uncertainty is practically negligible (since the π/e ratio and the pion asymmetry will be measured precisely).

If the processing of the FADC is fast enough we can maintain a deadtime which is very small, probably ≤ 10 nsec. However, the system may have a deadtime of order 1% which could be different for different physical processes. Our goal is to measure the deadtime correction to the physics asymmetry with an absolute accuracy $\pm 0.3\%$. To ensure reliability it is important to measure the deadtime with at least two independent methods as follows. A first method is to pulse the detector channels with a light sources whose amplitude and pulse shape is similar to those of real particles, and count how many of these signals are subsequently identified by the electronics. A second method is to introduce a deliberate programmed deadtime into the frontend, thus making it predictable and understood.

2. Scaler-based DAQ

An alternative way to count events is to use a customized set of conventional NIM modules to make detector coincidences read out by scaler modules. The electronics will process signals from PID detectors and scintillators and perform a fast on-line discrimination. Useful electrons, pions, and two-electron pileup events will be identified using different discrimination thresholds, see Fig. 6.

FIG. 6: PID Logic diagram for the scaler-based DAQ. The system will be replicated for several groups of lead glass detectors to provide information on W .



To ensure the stability of this scaler electronics, the outputs of a typical module need to be wide enough, typically 20 ns, causing a deadtime of 2.4% for 1.2 MHz rate. We plan to measure this deadtime also to an absolute accuracy of $\pm 0.3\%$ using the same methods as described above for the FADC DAQ. More importantly, it will provide a reliable online check of the FADC counting both for data taking at high rates and test runs at low rates. If any inconsistency is observed between the two DAQs, one can investigate possible problems promptly. For example, full-sampling FADC data can be collected to diagnose whether there is a problem with the FPGA algorithm.

IV. EXPECTED RESULTS

A. Kinematic Coverage

The kinematic coverage in W , Q^2 , x , and Y is shown in Table I. The full resonance region $M < W < 2.1$ GeV is covered, with an average Q^2 of 0.8 GeV² for $E = 4.8$ GeV. Figure 7 shows the distribution of events at the HRS calorimeter for the $P_{HRS} = 3.2$ GeV setting. With the FADC system, we will divide the calorimeter into four sections, yielding four W bins per setting, as indicated by the dashed lines in Fig. 7. Because the W bins are narrower for the low E' settings, we show projected results with four bins for the high HRS momentum settings, and two bins for the lower momentum settings. This yields approximately uniform bins in W , with an average FWHM below 90 MeV. The scaler-based DAQ could have even finer binning, providing better W resolution, but the resolution with four bins per setting is sufficient for the proposed measurements.

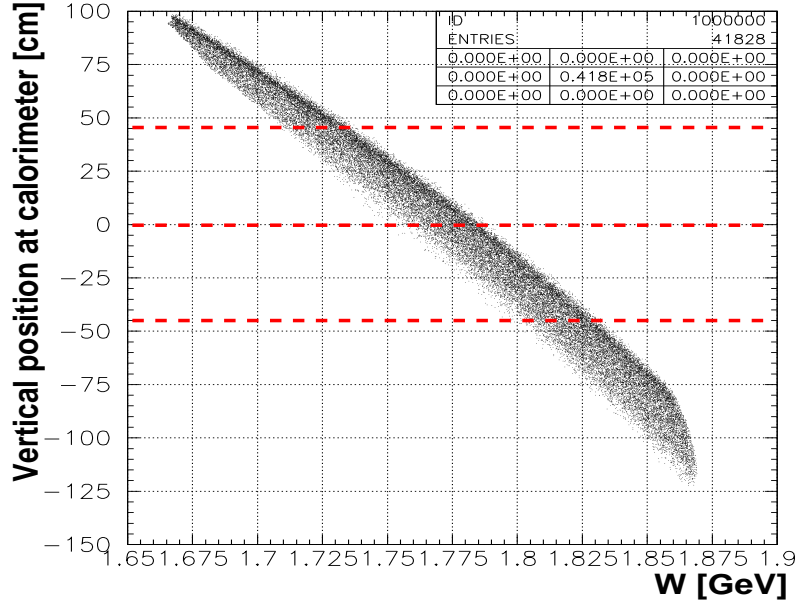


FIG. 7: Simulation for $E' = 3.2$ GeV, showing the vertical position of events at the calorimeter as a function of W . Dashed lines indicate the segmentation of the calorimeter for the FADC DAQ.

B. Statistical and Systematic Uncertainties

The expected statistical errors are listed in Table I. We will divide each spectrometer setting into two (or more) W bins. Resonant structure on the scale of 10% will be clearly visible with these data: this is small compared to the 30% to 50% resonant fluctuations of the unpolarized structure functions around the smooth duality curve. For tests of local duality, we can divide the full resonance region into four regions in W , and in each region will be able to test local duality at the level of about 4%. This seems quite adequate for a pioneering measurement. At these Q^2 values, duality in the unpolarized structure function is good to $\sim 5\%$, so this measurement will be able to determine if duality in parity violating electron scattering is of a similar quality or if there are significantly larger deviations. This information, coupled with recent measurements of duality in longitudinal, transverse, and spin-dependent structure functions will provide additional input to efforts aimed at understanding the origin of duality in QCD.

The statistical error for a test of global duality (averaged over the entire resonance region) will be at the level of 2%, which is well-matched to the anticipated systematic error (see below). The error on the ratio of averaged proton, deuteron, and carbon asymmetries will be about 3%, with a much smaller systematic error, since the largest sources of systematic uncertainty cancel in the ratio.

The expected systematic errors are tabulated in Table II, and discussed in the following sub-sections.

C. Beam Polarization

We will use the Hall A Compton polarimeter, as described in section IIIB. With the upgraded polarimeter being developed for PREX [59] and DIS-parity [52], we will achieve a 1.2% measurement of the beam polarization. The PREX experiment is planning an upgrade of the Møller polarimeter to achieve a 1% measurement. We will use this as a cross check for the Compton polarimeter if it is available in time.

TABLE I: Kinematic variables, pion/electron ratio, total particle rate (electron plus pion), expected asymmetry (DIS model), and expected asymmetry error for the proposed measurements. All entries are for a beam energy of 4.8 GeV and an electron scattering angle $\theta_e = 12.5^\circ$.

W (GeV)	x	Q^2 (GeV ²)	Y	E' (GeV)	π/e	rate (MHz)	A (ppm)	dA_{stat} (ppm)	dA_{total} (ppm)
LH2									
2.00	0.17	0.64	0.50	3.0	0.5	0.5	46	3.2	3.3
1.78	0.24	0.73	0.39	3.2	0.2	0.5	51	3.3	3.4
1.52	0.36	0.82	0.29	3.6	0.1	0.6	53	2.3	2.5
1.21	0.61	0.91	0.19	4.0	0.0	0.8	52	2.2	2.4
LD2									
2.00	0.17	0.64	0.50	3.0	0.6	0.8	61	2.7	2.9
1.78	0.24	0.73	0.39	3.2	0.2	0.9	64	2.3	2.6
1.52	0.36	0.82	0.29	3.6	0.1	0.9	67	2.1	2.5
1.21	0.61	0.91	0.19	4.0	0.0	1.3	71	1.7	2.1
Carbon									
2.00	0.17	0.64	0.50	3.0	0.6	0.5	61	2.8	3.0
1.78	0.24	0.73	0.39	3.2	0.2	0.5	64	2.4	2.7
1.52	0.36	0.82	0.29	3.6	0.1	0.5	67	2.3	2.6
1.21	0.61	0.91	0.19	4.0	0.0	0.9	71	1.8	2.2

TABLE II: Estimated experimental systematic errors on dA/A . Note that in the comparison of proton, deuteron, and carbon, the uncertainties in the beam polarization and Q^2 determination will largely or completely cancel, yielding a systematic of ≈ 0.010 for the target ratios.

source	$\delta A/A$
Beam Polarization	0.012
Kinematic determination of Q^2	0.009
Electromagnetic radiative corrections	0.008
Beam asymmetries	0.005
Pion contamination	0.005
Deadtime corrections	0.003
Pair symmetric background	0.002
Target purity, density fluctuations	0.002
Poletip background	0.001
Total	0.019

D. Kinematic determination of Q^2

Since the raw asymmetry has a linear dependence on Q^2 , but a small dependence on other kinematic variables such as W or x , the largest systematic error in the physics asymmetry determination arises from the knowledge of the average Q^2 of the events seen in each detector, weighted by detector response. The average Q^2 will be determined from a detailed model of the spectrometer apertures and magnetic fields. The HRS spectrometers are very well understood from previous experiments, and preliminary studies indicate that we will be able to determine the average Q^2 value, to better than 0.9%. The

asymmetry is proportional to Q^2 , yielding a systematic uncertainty in A of $< 0.9\%$.

The uncertainty in beam energy E is $< 0.02\%$, which contributes a negligible uncertainty to $Q^2 = 4EE' \sin^2(\theta/2)$. The HRS central momentum is known to $< 0.1\%$, and the central angle can be determined to better than 1 mr. These generate an uncertainty in the central Q^2 value of less than 0.9% , dominated by the uncertainty in the scattering angle. Previous experiments have determined the HRS angle to better than 0.5 mr, which would yield an uncertainty in Q^2 of 0.5% from this source. We will measure the electron rates as a function of all spectrometer variables with dedicated low rate running to check the geometric acceptance of the spectrometer to better than 0.9% , and will use the positions of the ep and ed elastic peaks as a cross check on the central angle and momentum of the spectrometers.

E. Electromagnetic Radiative Corrections

Electromagnetic radiative corrections arise from the emission of photons by either the incident or scattered electron, either in the field of the nucleus (internal corrections), or in the field of another nucleus (external corrections). The ratio R_U of un-radiated to radiated spin-averaged cross sections is shown in Fig. 8 for the kinematics of the proposed measurements. At high W (low electron momentum P), the radiated cross section is larger than the Born cross section, while the reverse is true at high W . In the kinematics of this proposal, R_U is mainly determined by the (x, Q^2) dependence of the spin-averaged structure function F_2 . Of particular relevance is the ratio R_P of radiated to un-radiated ed parity-violating asymmetry. This ratio is close to unity for the kinematics of this proposal. The shape and magnitude of R_P is primarily determined by the probability for an electron to radiate a hard photon, and to a lesser extent by the (x, Q^2) dependence of F_2 and A_p . We have estimated the systematic error in A_p , A_d , and A_C to be about 0.5% to 0.8% over most of the kinematics of this experiment by considering the uncertainty in the unpolarized cross section (using several fits to world data) and in A_p , which will be largely determined by an iterative fit to the data of this proposal (although the elastic contributions to A_p are already reasonably well known from previous experiments). Uncertainties in the target dimensions and various materials which act as radiators have much smaller effects. These calculations were performed in the peaking approximation of Mo and Tsai [69–71]. Calculations with the more exact formulas of Ref. [72, 73] are planned.

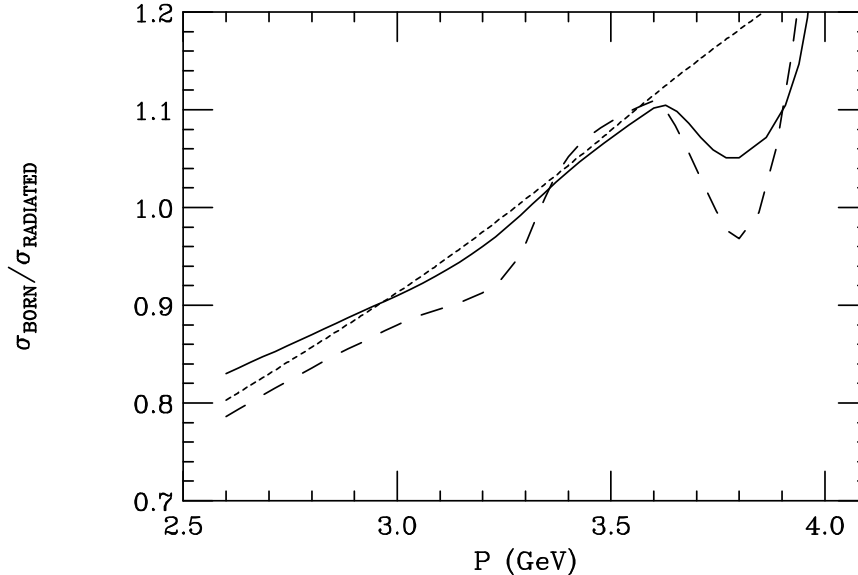


FIG. 8: Radiative correction as a function of scattered electron momentum P for $E = 4.8$ GeV. The curves are for deuterium (solid), proton (long dash), and carbon (short dashed).

F. Electroweak Radiative Corrections

Interpretation of the experimental results in terms of transition form factors (both axial and vector) requires the careful treatment of electroweak radiative corrections. In the case of the $\Delta(1232)$ resonance, these can be sizable, and increase in relative importance as $Q^2 \rightarrow 0$ [74]. We are not aware of calculations for higher mass resonances. For the interpretation of the data in terms of quark-hadron duality, and for simply searching for resonance structure in A_p , it is not crucial to have a complete understanding of electroweak radiative corrections, so we haven't included an uncertainty in the systematic error table. However one should keep in mind their importance in the interpretation of the data in terms of specific transition form factors.

G. Beam Asymmetries

Since the raw asymmetry in this experiment is 50 to 1000 times larger than other JLab PV experiments, our requirements on beam position, angle, energy, and charge asymmetries are relatively modest. Using the parity DAQ and the luminosity monitor as described in sections III C and III E, we are confident that the false asymmetry due to beam quality will be under control, and the uncertainty will be negligible compared to the statistical uncertainty of the proposed measurement.

We will periodically reverse the half-wave plate at the injector to help cancel any residual false asymmetries.

H. Pion Contamination

The sign and magnitude of the pion asymmetry is of some physics interest in its own right, especially as it may impact backgrounds in experiments such as E158 and G0. It was seen to be small in the original SLAC experiment [1, 2]. While we don't know of any calculations of the pion photoproduction asymmetry at our kinematics, the predicted asymmetry is of order 10^{-7} at energies below 0.55 GeV [75], and 1.3×10^{-6} for excitation of the $\Delta(1232)$ resonance [76]. These are both negligible compared to our expected electron asymmetry of about 1×10^{-4} .

The predicted π/e ratios shown in Table I are based on a fit to pion photoproduction data [77], which has proved to be accurate to 30% or better in past experiments. The π/e ratio is strongly W -dependent, approaching 1 in the highest W bin. We will measure both pions and electrons (see sections III G and III H) during each run, yielding a measure of the pion asymmetry for each setting. The π/e ratio will be measured precisely using the regular HRS DAQ at low rates. Because the pion asymmetry is expected to be negligible compared to the electron asymmetry, only the dilution is expected to be important. With the proposed particle identification cuts, the pion contamination should be $< 1\%$ to the electron sample (mainly due to pileup) for all kinematic conditions. Because we will have a good measure of the pion and electron rates, we can correct for this with a systematic uncertainty below 0.5%.

I. Pair Symmetric Background

In addition to the electron scattering events of interest, electrons can originate from decays of vector and pseudo-scalar mesons, and wide angle pair production. To a very good approximation, these processes are pair-symmetric, and can be measured with better than 3% accuracy by reversing the polarity of the spectrometers. Based on simulations with PYTHIA [78], we expect the largest source of pair-symmetric events to be from decays of photoproduced π^0 mesons. The simulation is in reasonable agreement with data taken in Halls B and C over the past years. The highest predicted e^+/e^- ratio for this proposal is about 0.5% (at $W = 2.1$ GeV), and drops rapidly at lower W . The asymmetry is expected to be very small, and this will be verified by taking data for a few hours with reversed spectrometer polarity. The net relative uncertainty on A_p and A_d will be $< 0.2\%$.

TABLE III: Beam time request. All data taken with 4.8 GeV beam and both HRS spectrometers at 12.5° .

Target	P (HRS-L)	P (HRS-R)	time
LH2	4.0 GeV	3.2 GeV	5 days
LH2	3.6 GeV	2.8 GeV	4 days
LD2	4.0 GeV	3.2 GeV	4 days
LD2	3.6 GeV	2.8 GeV	4 days
Carbon	4.0 GeV	3.2 GeV	6 days
Carbon	3.6 GeV	2.8 GeV	6 days
Pass Change			8 hours
Polarimetry runs			8 hours
e^+ Asymmetry			8 hours
Total			30 days

J. Target Related Systematics

Target boiling effects are expected to be very small for the proposed 25 cm LH2 and LD2 targets and $85 \mu A$. The increase in effective statistical fluctuations should be negligible, as described in section III D. In addition, the small-angle luminosity monitor will be used to verify a null asymmetry, as described in section III E, and provide additional confidence that target density fluctuations and helicity-correlated beam asymmetries are small.

With a magnetic field at the target of < 10 Gauss, the proton polarization will be less than 0.001%, leading to a negligible double-spin asymmetry from the g_1 structure function.

Impurities in the liquid hydrogen are typically less than 0.1%, and are expected to cause a negligible effect on A_p since the asymmetry has only a weak dependence on atomic number A . The largest effect will be from the aluminum endcaps, for which the asymmetry is typically 20% larger than for the proton is the DIS limit. Since the endcaps contribute only a few percent of the count rate, this correction is small, and will be constrained by the carbon asymmetry measurements, for which the asymmetry should be nearly identical to aluminum (after making a small neutron excess correction based on the proton and deuteron measurements). For the deuteron measurements, the biggest correction comes from the fraction of hydrogen. This will be measured to better than 0.2%, leading to a negligible systematic error on A_d .

V. REQUEST

We request 29 days of production data and one day for checkout, Møller beam polarization measurements (Compton measurements are done concurrently with production data taking), and configuration changes, as summarized in Table III. While 4.8 GeV is optimal, energies between 4.6 and 5.2 GeV would be acceptable, yielding slightly reduced statistics at the lower energy and introducing a slight gap in the W coverage at increased energies.

This experiment requires only standard Hall A equipment, with the exception of the upgraded Compton polarimeter being developed for several experiments, the target configuration (same as for E05-007 with the possible addition of one more liquid target cell to facilitate alternating between LH2 and LD2), and the high speed DAQ system which is presently being built for the DIS-parity measurement E05-007. We will work with the E05-007 collaboration on the implementation of the necessary equipment. Our run time request assumes sequential or interleaved running with E05-007, which has already allocated 4 of the 13 approved PAC days for checkout and commissioning of the new target and DAQ systems, Q^2 measurements, checkout of the upgraded Compton polarimeter, and particle identification checks with low current beam. Since the π/e ratio is lower for our proposed kinematics than for E05-007, the incremental time to check pion and pair symmetric background is relatively small for the present

proposal. We main change in going from one experiment to the other is simply a change from 5-pass to 4-pass running.

Figures 9 and 10 show the projected uncertainties for the asymmetries for each target as a function of ξ and W .

VI. PHYSICS SUMMARY

This experiment will provide the first measurements of the PV asymmetry in inelastic electron scattering from the proton and deuteron in the resonance region beyond the $\Delta(1232)$. The precision will be sufficient to observe resonance structure at the 5% to 10% level, and to test local and global duality at the few percent level, comparable to the level at which duality is observed in the unpolarized structure functions. The PV asymmetry is also useful because it is more sensitive to the down and strange quarks than the unpolarized structure functions, allowing us to study the d/u ratio in the proton without the nuclear corrections that enter when studying the neutron in nuclear targets.

Data on deuterium and carbon will allow us to look for nuclear dependence in the PV asymmetry. Recent measurements of the nuclear dependence of F_2 in the resonance region show nearly identical effects to the EMC measurements in the DIS limit [47], while recent calculations show that medium modifications may be very different in spin-averaged and spin-dependent structure functions, with a significant dependence on quark flavor [55].

The results will not only be interesting in their own right as a new way to probe the fundamental structure functions of the proton and neutron, but will be of great value in the growing world-wide program of neutrino studies. The new data will also provide details about the backgrounds in other PV experiments, and are needed as input to DIS-parity studies at 6 and 11 GeV through radiative corrections.

VII. COLLABORATION

The collaboration has many members with recent experience in precision electron PV experiments (such as SLAC E158 and JLab HAPPEX), and we are confident that we will be able to control systematic errors at the few percent level. The collaboration has large overlap with the DIS-parity collaboration that is working on the upgrades to the Compton polarimeter and the fast data acquisition system.

Appendix A. E04-101: G0 Backward Angle Measurement

This proposal had no abstract, so we here reproduce a portion of the Introduction, which gives a good overview of the experiment: “In this experiment, the parity violating asymmetry in inclusive single pion electroproduction from the proton will be measured over a squared four momentum transfer range of $0.1 \leq Q^2 \leq 0.6$ (GeV/c)². These measurements will be made with the same equipment as the G0 backward angle measurements are made, and during the same running period as the G0 backward angle measurements, so that no additional resources or beam time are required beyond those allocated for G0 backward angle running. The primary purpose of this experiment is to extract the axial vector transition form factor $G_{N\Delta}^A$ for the $N \rightarrow \Delta$ transition as a function of Q^2 . This form factor characterizes the axial, or intrinsic spin response of the nucleon during its transition to its first excited state. The proposed measurements represent the first determination of this quantity in the neutral current sector of the weak interaction, and in a Q^2 range that is complementary to other experiments (with Q^2 coverage $0.5 \leq Q^2 \leq 2.5$ (GeV/c)²) which use exclusive electroproduction of the Δ^{++} resonance, along with assumptions of PCAC and extrapolations of low energy theorems, to extract the charged current analog of this form factor. In addition to the extraction of $G_{N\Delta}^A$, these measurements of the inelastic asymmetry will constrain the contribution of inelastic electrons to the elastic parity violating asymmetry, which is the primary goal of the G0 program.”

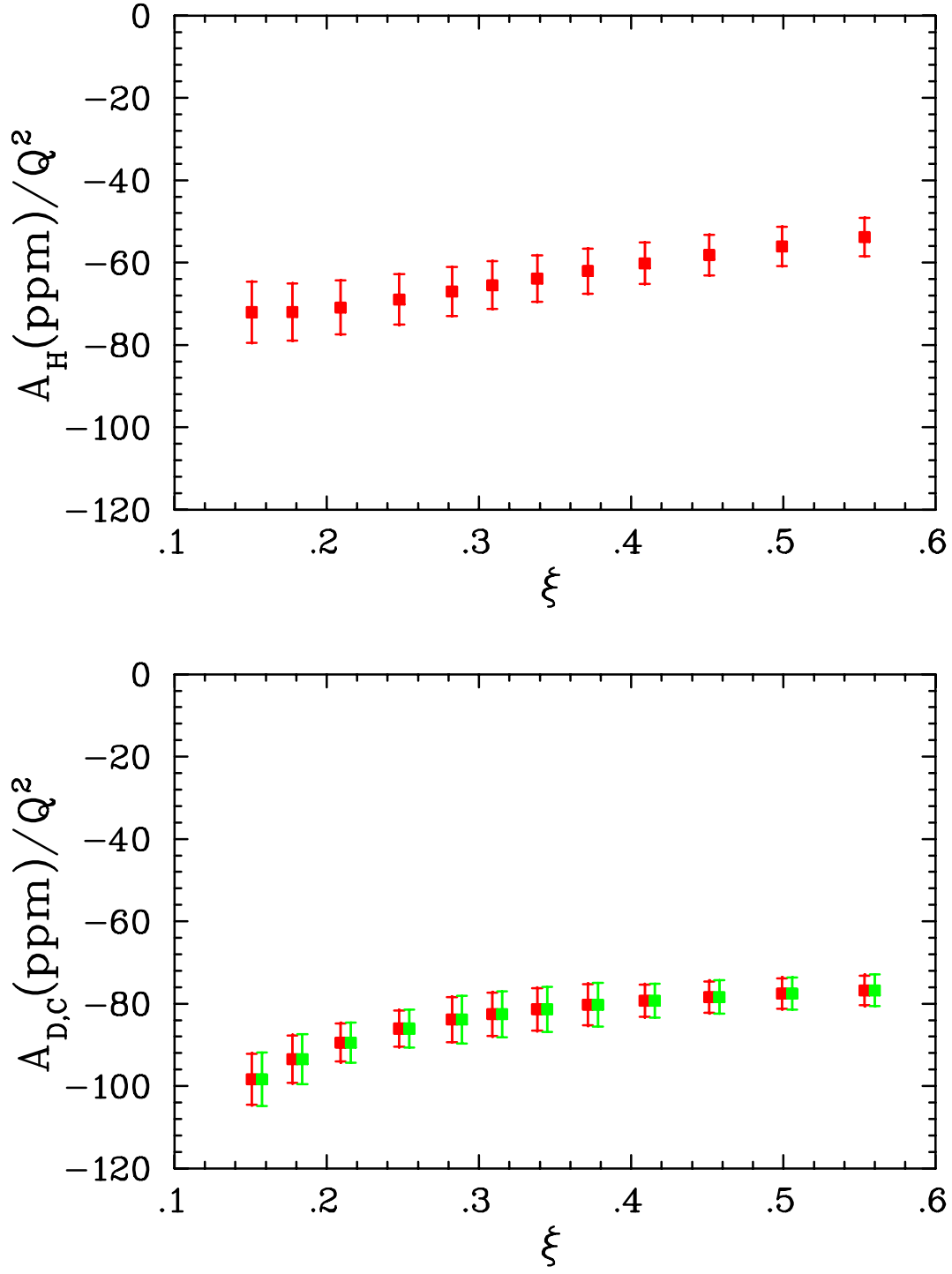


FIG. 9: Projected errors for the PV asymmetry divided by Q^2 (in ppm/GeV²) as a function of ξ , plotted along the DIS model prediction. The top figure is for hydrogen, while the bottom figure shows the projected uncertainties for deuterium (red) and carbon (green, shown slightly offset in ξ). Each spectrometer setting has been divided into two or four W bins. The error bars shown include both statistical and systematic (<2%) uncertainties.

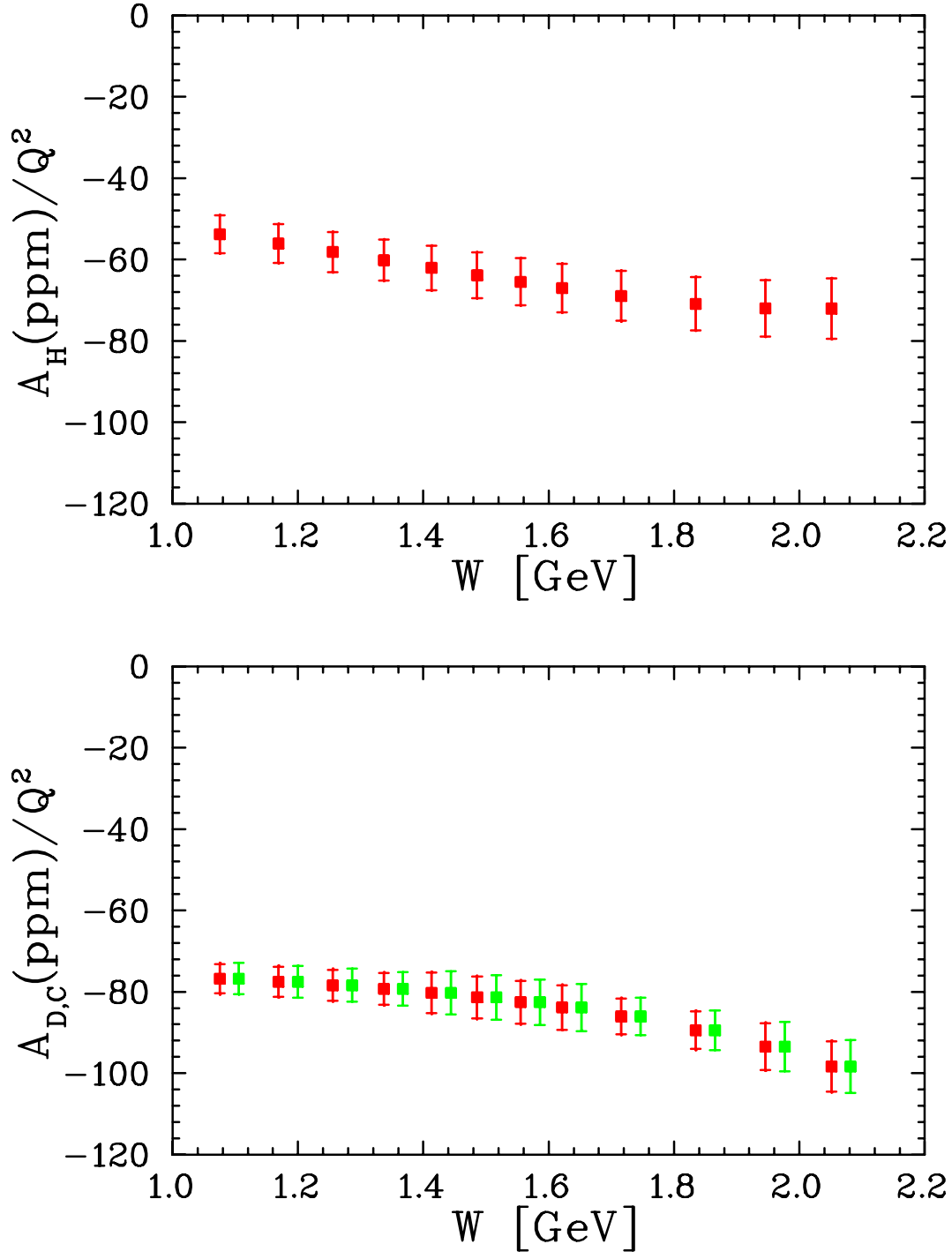


FIG. 10: Projected results (as in Fig. 9), shown as a function of W .

The Q^2 range of the experiment will be somewhat reduced, because G0 is now planning to run at a maximum beam energy of 0.68 GeV instead of 0.8 GeV.

Appendix B. E05-007: \bar{e} - ^2H Parity Violating Deep Inelastic Scattering at CEBAF 6 GeV

Here is the abstract of this experiment, for which Phase I has been approved:

“We propose to measure the parity violating (PV) asymmetry A_d in \bar{e} - ^2H deep inelastic scattering (DIS) at $Q^2 = 1.1$ and 1.9 GeV^2 at similar x . The main goal is to extract the effective coupling constants $(2C_{2u} - C_{2d})$ from A_d measured at $Q^2 = 1.9 \text{ GeV}^2$. Using the Standard Model values of $(2C_{1u} - C_{1d})$, which will be tested by combining the results from Cs atomic parity violation (APV) and the future Qweak experiment, the expected uncertainty on $(2C_{2u} - C_{2d})$ is ± 0.03 . This result will improve the current knowledge on this quantity by a factor of eight. It will help to extract couplings C_{3q} from high energy data, and might reveal possible physics beyond the Standard Model.

The most probable effect that could cause a deviation of our measured asymmetry from its Standard Model value are higher-twist (HT) effects. If this is the case, then the proposed measurement at $Q^2 = 1.1 \text{ GeV}^2$ will have twice as large deviation from the SM. Thus this lower Q^2 measurement will secure the measurement at $Q^2 = 1.9 \text{ GeV}^2$. It will also for the first time probe and constrain the HT effects in parity violating electron scattering, thus will provide an important guidance on the future DIS-parity program with the 12 GeV upgrade, of which the ultimate goal is to extract $\sin^2 \theta_W$ from the asymmetry free from hadronic effects. On the other hand, if the higher-twist effects are observed to be non-negligible, in contrast to available calculations, then it may shed light on how much the higher-twist effect contributes to the 3σ anomaly observed by the NuTeV collaboration. At last, a precision measurement of the higher-twist itself would provide information on the study of confinement mechanism. An immediate application of such data is that they can be used in the extraction of the strong coupling constant α_s from DIS data at low Q^2 , whose present theoretical uncertainty is dominated by the uncertainty of the poorly-known higher-twist effects.

We plan to use a 25-cm liquid deuterium target in Hall A and a $85\mu\text{A}$ 6-GeV beam with 80% polarization. An upgrade is needed for the Compton polarimeter and a fast counting data acquisition system will be used by the proposed measurement. We request 46 days of beam time consisting of two phases: 13 days for phase I, and 33 days for phase II.”

-
- [1] C. Y. Prescott et al., Phys. Lett. **B77**, 347 (1978).
 - [2] C. Y. Prescott et al., Phys. Lett. **B84**, 524 (1979).
 - [3] Y. Liang et al. (2004), nucl-ex/0410027.
 - [4] O. Rondon-Aramayo et al., Jefferson lab experiment E01-006.
 - [5] A. De Rujula, H. Georgi, and H. D. Politzer, Ann. Phys. **103**, 315 (1977).
 - [6] E. D. Bloom and F. J. Gilman, Phys. Rev. Lett. **25**, 1140 (1970).
 - [7] C. E. Carlson and N. C. Mukhopadhyay, Phys. Rev. Lett. **74**, 1288 (1995).
 - [8] W. Melnitchouk, R. Ent, and C. Keppel, Phys. Rept. **406**, 127 (2005).
 - [9] K. Matsui, T. Sato, and T. S. H. Lee, Phys. Rev. **C72**, 025204 (2005).
 - [10] F. E. Close and N. Isgur, Phys. Lett. **B509**, 81 (2001).
 - [11] M. Hirai, S. Kumano, and M. Miyama, Phys. Rev. **D64**, 034003 (2001).
 - [12] M. Hirai, S. Kumano, and T. H. Nagai, Phys. Rev. **C70**, 044905 (2004).
 - [13] S. A. Kulagin and R. Petti (2004), hep-ph/0412425.
 - [14] G. P. Zeller et al. (NuTeV), Phys. Rev. Lett. **88**, 091802 (2002).
 - [15] G. P. Zeller et al. (NuTeV), Phys. Rev. **D65**, 111103 (2002).
 - [16] S. A. Kulagin, Phys. Rev. **D67**, 091301 (2003).
 - [17] M. Hirai, S. Kumano, and T. H. Nagai, Nucl. Phys. Proc. Suppl. **149**, 224 (2005).
 - [18] D. A. Harris et al. (MINERvA) (2004), hep-ex/0410005.
 - [19] A. Bodek, I. Park, and U.-k. Yang, Nucl. Phys. Proc. Suppl. **139**, 113 (2005).
 - [20] K. Graczyk, C. Juszczak, and J. Sobczyk, (2005), hep-ph/0512015.
 - [21] E. A. Paschos and J. Y. Yu, Phys. Rev. **D65**, 033002 (2002).

- [22] E. A. Paschos, J.-Y. Yu, and M. Sakuda, Phys. Rev. **D69**, 014013 (2004).
- [23] E. A. Paschos, M. Sakuda, I. Schienbein, and J. Y. Yu, Nucl. Phys. Proc. Suppl. **139**, 125 (2005).
- [24] S. Kretzer and M. H. Reno, Phys. Rev. **D66**, 113007 (2002).
- [25] R. Belusevic and D. Rein, Phys. Rev. **D38**, 2753 (1988).
- [26] C. E. Carlson and N. C. Mukhopadhyay, Phys. Rev. **D47**, 1737 (1993).
- [27] M. J. Musolf et al., Phys. Rept. **239**, 1 (1994).
- [28] J. E. Amaro, M. B. Barbaro, J. A. Caballero, T. W. Donnelly, and A. Molinari, Phys. Rept. **368**, 317 (2002).
- [29] M. B. Barbaro, J. A. Caballero, T. W. Donnelly, and C. Maieron, Phys. Rev. **C69**, 035502 (2004).
- [30] A. De Pace, M. Nardi, W. M. Alberico, T. W. Donnelly, and A. Molinari, Nucl. Phys. **A741**, 249 (2004).
- [31] S. L. Adler, Ann. Phys. **50**, 189 (1968).
- [32] R. N. Cahn and F. J. Gilman, Phys. Rev. **D17**, 1313 (1978).
- [33] D. R. T. Jones and S. T. Petcov, Phys. Lett. **B91**, 137 (1980).
- [34] L. M. Nath, K. Schilcher, and M. Kretschmar, Phys. Rev. **D25**, 2300 (1982).
- [35] G. F. Sacco, Ph.D. thesis, University of Connecticut (2004).
- [36] J. Blumlein et al., HERA Workshop Vol. 1, p. 69, Hamburg 1989.
- [37] J. Erler and P. Langacker, Phys. Rev. **D66**, 010001 (2002).
- [38] M. K. Jones, private communication.
- [39] T. Forest, K. Johnston, N. Simicevic, S. Wells, et al., Jefferson lab experiment E04-101.
- [40] I. Niculescu et al., Phys. Rev. Lett. **85**, 1186 (2000).
- [41] T. Sato and T. S. H. Lee, Phys. Rev. **C54**, 2660 (1996).
- [42] T. Sato and T. S. H. Lee, Phys. Rev. **C63**, 055201 (2001).
- [43] T. Sato, D. Uno, and T. S. H. Lee, Phys. Rev. **C67**, 065201 (2003).
- [44] T. S. H. Lee, private communication.
- [45] B. W. Filippone et al., Phys. Rev. C **45**, 1582 (1992).
- [46] J. Arrington et al., Phys. Rev. C **64**, 014602 (2001).
- [47] J. Arrington, R. Ent, C. E. Keppel, J. Mammei, and I. Niculescu (2003), nucl-ex/0307012.
- [48] G. Ricco, M. Anghinolfi, M. Ripani, S. Simula, and M. Taiuti, Phys. Rev. C **57**, 356 (1998).
- [49] I. Niculescu, J. Arrington, R. Ent, and C. E. Keppel (2005), hep-ph/0509241.
- [50] P. Castorina and P. J. Mulders, Phys. Rev. **D31**, 2760 (1985).
- [51] S. Fajfer and R. J. Oakes, Phys. Rev. **D30**, 1585 (1984).
- [52] R. Michaels, P. E. Reimer, X. Zheng, et al., Jefferson lab experiment E93-027.
- [53] M. Virchaux and A. Milsztajn, Phys. Lett. **B274**, 221 (1992).
- [54] M. Gluck and E. Reya, Phys. Rev. Lett. **47**, 1104 (1981).
- [55] I. C. Cloet, W. Bentz, and A. W. Thomas, Phys. Rev. Lett. **95**, 052302 (2005).
- [56] J. R. Smith and G. A. Miller, Phys. Rev. **C72**, 022203 (2005).
- [57] P. L. Anthony et al. (SLAC E158), Phys. Rev. Lett. **95**, 081601 (2005).
- [58] J. Alcorn et al., Nucl. Inst. & Meth. **A522**, 294 (2004).
- [59] R. Michaels et al., “*Neutron skin of ^{208}Pb Through Parity Violating Electron Scattering*”, Jefferson lab experiment E03-001.
- [60] K. A. Aniol et al. (HAPPEX), Phys. Rev. **C69**, 065501 (2004).
- [61] D. S. Armstrong, presentation at the Feb. 18 2005 HAPPEX collaboration meeting: hallaweb.jlab.org/experiment/HAPPEX/minutes/05Feb18/DSA_boil.pdf.
- [62] H. Ibrahim, P. Ulmer, and N. Liyanage, Tech. Rep., Hall A Technical Note JLAB-TN-02-032 (2002).
- [63] P. Souder, Tech. Rep., HAPPEX Technical Note (1998).
- [64] X. Zheng, “*JLAB Hall A detector PID efficiency analysis using high electron and high pion rate data*”, hallaweb.jlab.org/physics/experiments/he3/A1n.
- [65] D. v. Harrach, F. E. Mass, et al., <http://www.kph.uni-mainz.de/A4>.
- [66] S. Koebis, P. Achenbach, et al., Nucl. Phys. B (Proc. Suppl.) **61B**, 625 (1998).
- [67] G. Batigne et al., “*Deadtime Corrections for the French Electronics*”, G0 Internal Memo.
- [68] X. Zheng “*Full FADC/FPGA Algorithm for E05-007*”, http://www.jlab.org/xiaochao/pvdis/daq/daq_algorithm.pdf.
- [69] L. W. Mo and Y.-S. Tsai, Rev. Mod. Phys. **41**, 205 (1969).
- [70] Y. S. Tsai, Tech. Rep., SLAC Report (1971).
- [71] Y.-S. Tsai, Rev. Mod. Phys. **46**, 815 (1974).
- [72] D. Y. Bardin and N. M. Shumeiko, Sov. J. Nucl. Phys. **29**, 499 (1979).
- [73] D. Y. Bardin, P. K. Khristova, and O. M. Fedorenko, Nucl. Phys. **B197**, 1 (1982).
- [74] S.-L. Zhu, C. M. Maekawa, G. Sacco, B. R. Holstein, and M. J. Ramsey-Musolf, Phys. Rev. **D65**, 033001 (2002).
- [75] S. P. Li, E. M. Henley, and W. Y. P. Hwang, Annals Phys. **143**, 372 (1982).

- [76] S.-L. Zhu, C. M. Maekawa, B. R. Holstein, and M. J. Ramsey-Musolf, Phys. Rev. Lett. **87**, 201802 (2001).
- [77] D. E. Wiser, Ph.D. thesis, University of Wisconsin (1977).
- [78] T. Sjostrand, Comput. Phys. Commun. **82**, 74 (1994).